

Electronic Supporting Information

Synthesis and Structure-property Investigation of Multi-arm Oligothiophenes

*Choong Ping Sen and Suresh Valiyaveetil**

Department of Chemistry, National University of Singapore, Singapore.

*chmsv@nus.edu.sg

Table of Contents

1. ^1H and ^{13}C NMR and mass spectra
2. DSC results
3. Optimized structures and frontier orbital plots of SCTs
4. Absorption and emission spectra of SCTs in presence of Pb(II) and Cd(II) ions.
5. Absorption spectra of SCT-4 at pH 1 - 6
6. SEM micrographs on SCT/Hg(II) and SCT/TCNQ complexes
7. Theoretical calculations on HOMO energy levels of SCTs

1. ^1H , ^{13}C NMR and mass spectra

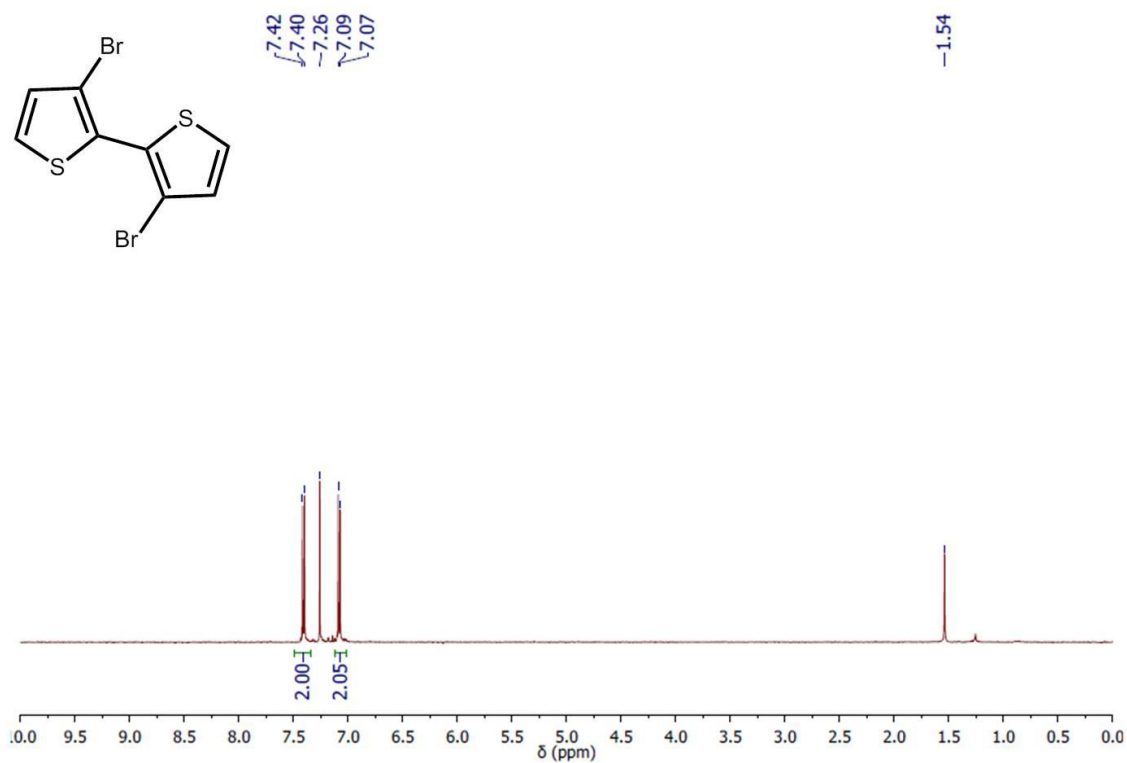


Figure S1. ^1H NMR spectrum of compound **1** in CDCl_3 .

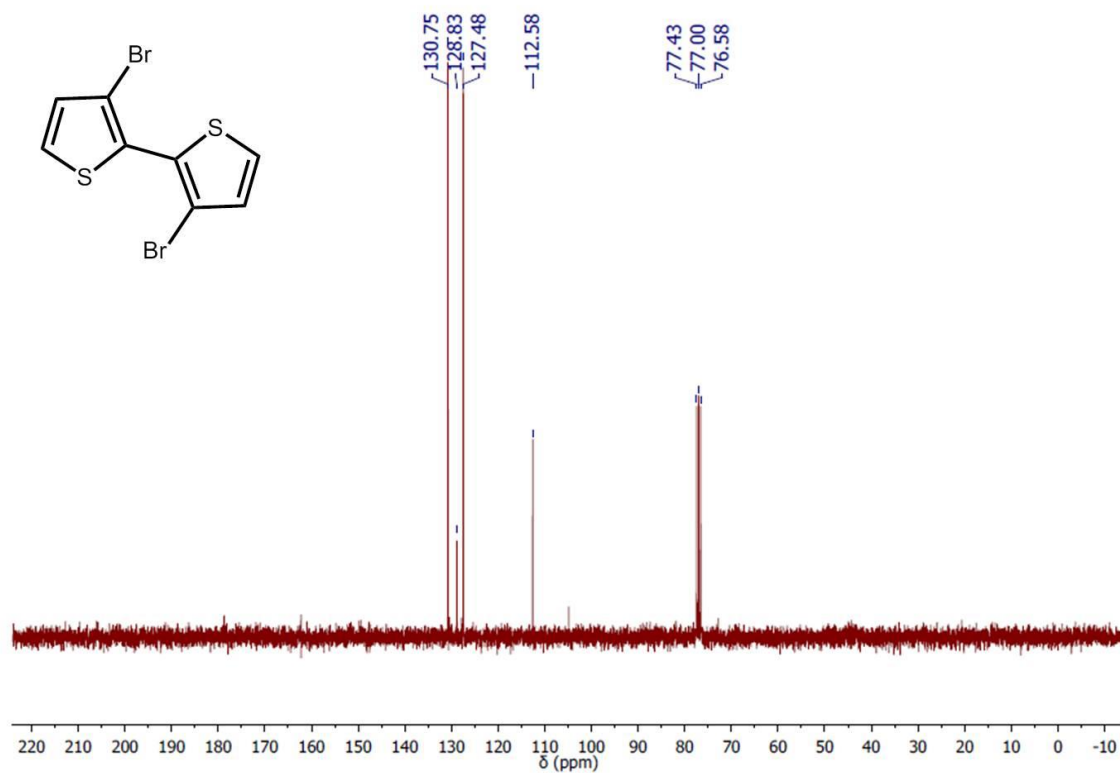


Figure S2. ^{13}C NMR spectrum of compound **1** in CDCl_3 .

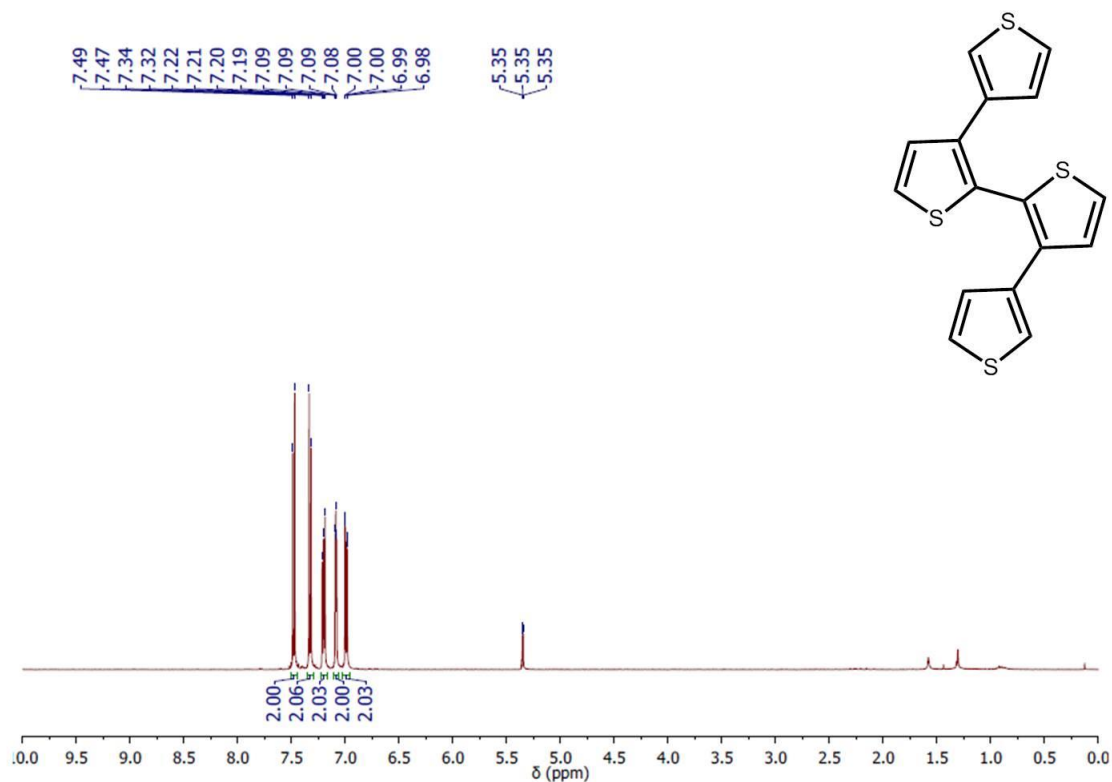


Figure S3. ^1H NMR spectrum of compound **2** in CD_2Cl_2 .

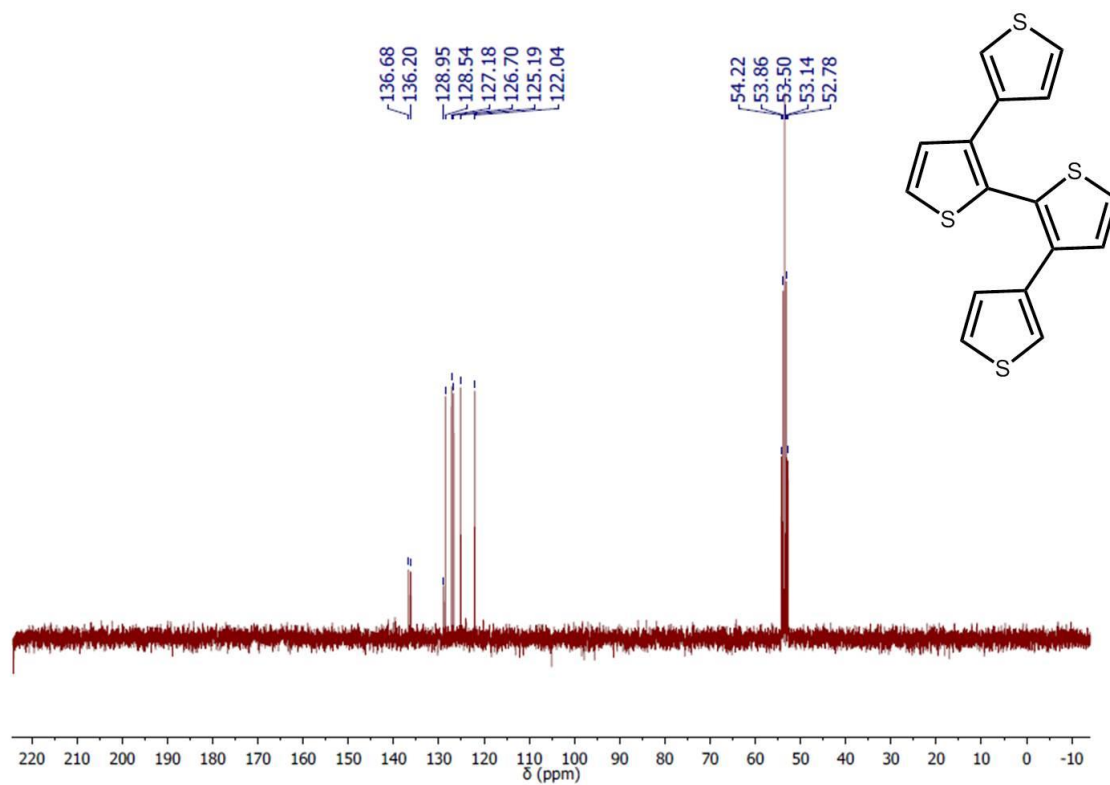


Figure S4. ^{13}C NMR spectrum of compound **2** in CD_2Cl_2 .

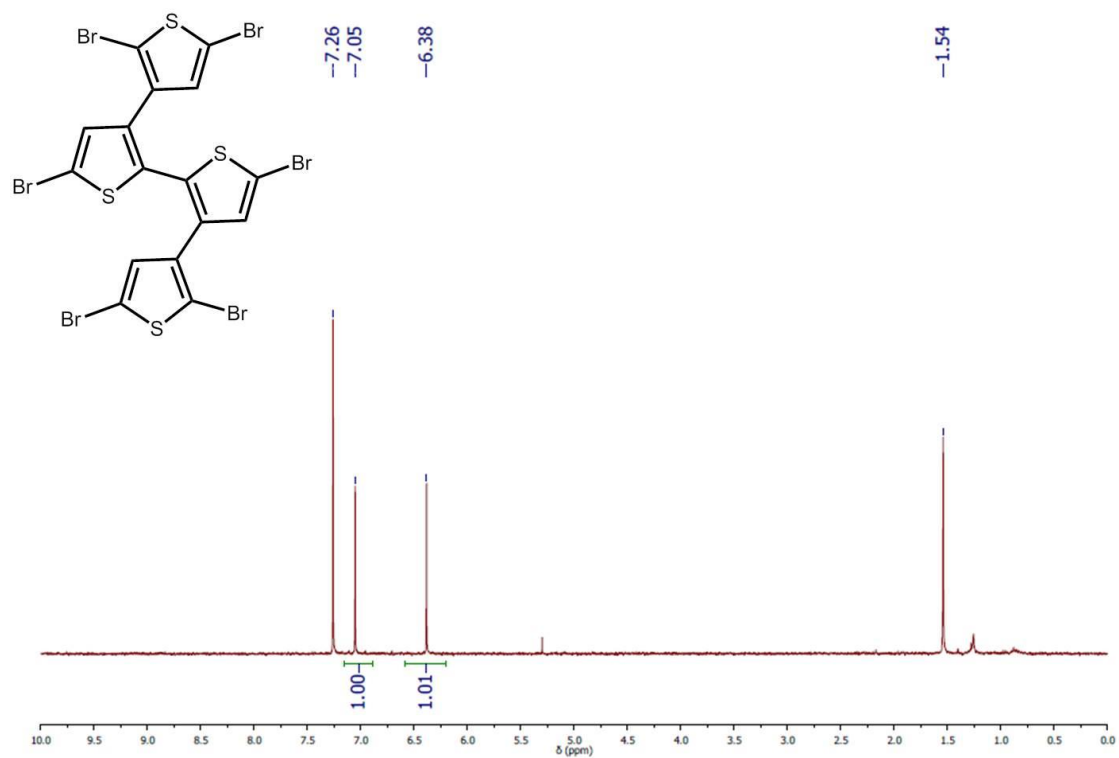


Figure S5. ^1H NMR spectrum of compound **3** in CDCl_3 .

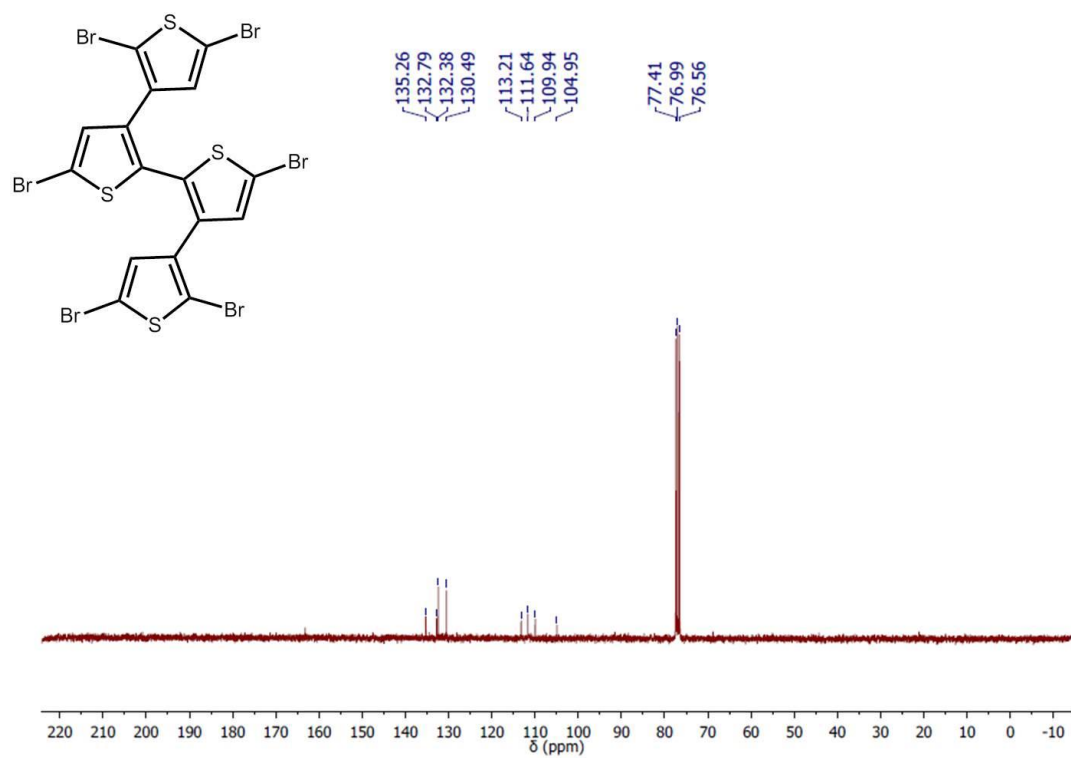


Figure S6. ^{13}C NMR spectrum of compound **3** in CDCl_3 .

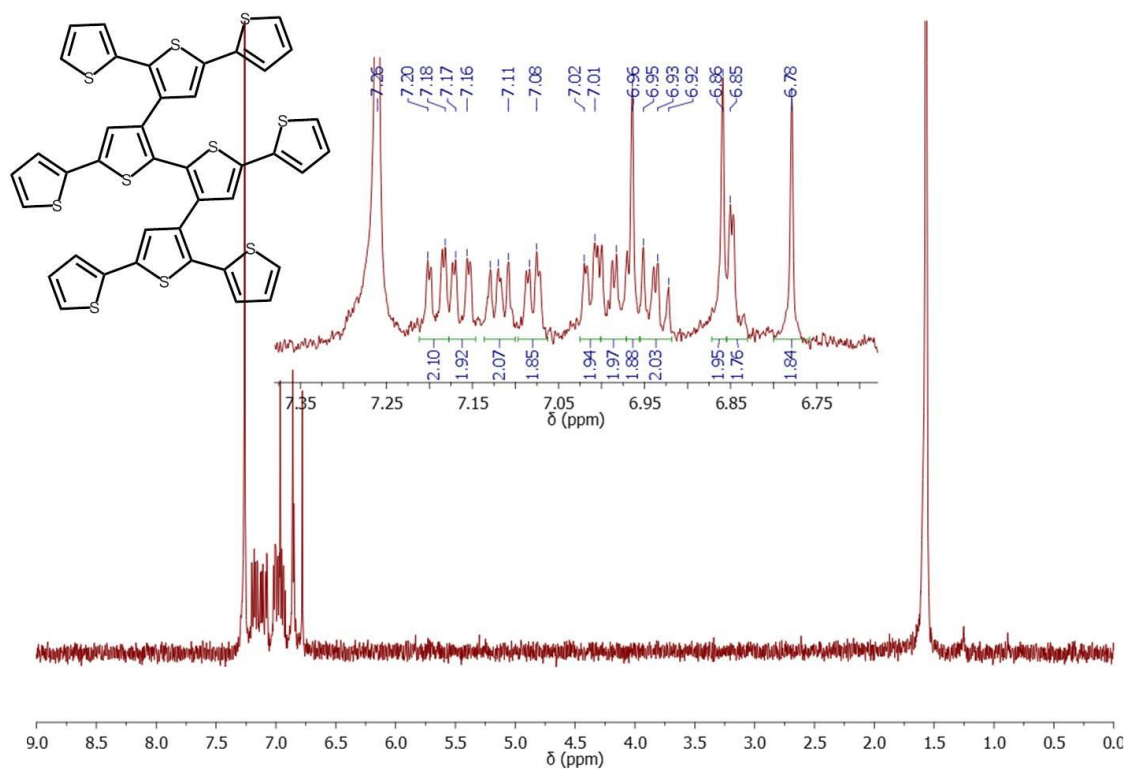


Figure S7. ¹H NMR spectrum of SCT-1 in CDCl₃.

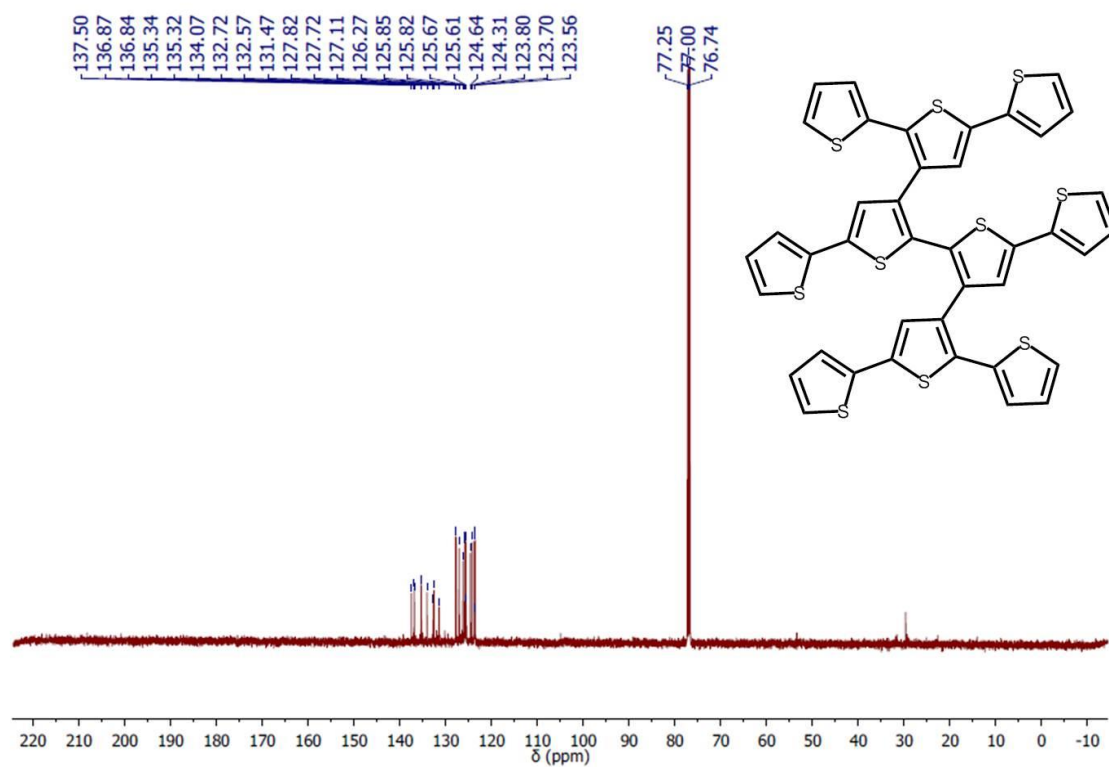


Figure S8. ¹³C NMR spectrum of SCT-1 in CDCl₃.

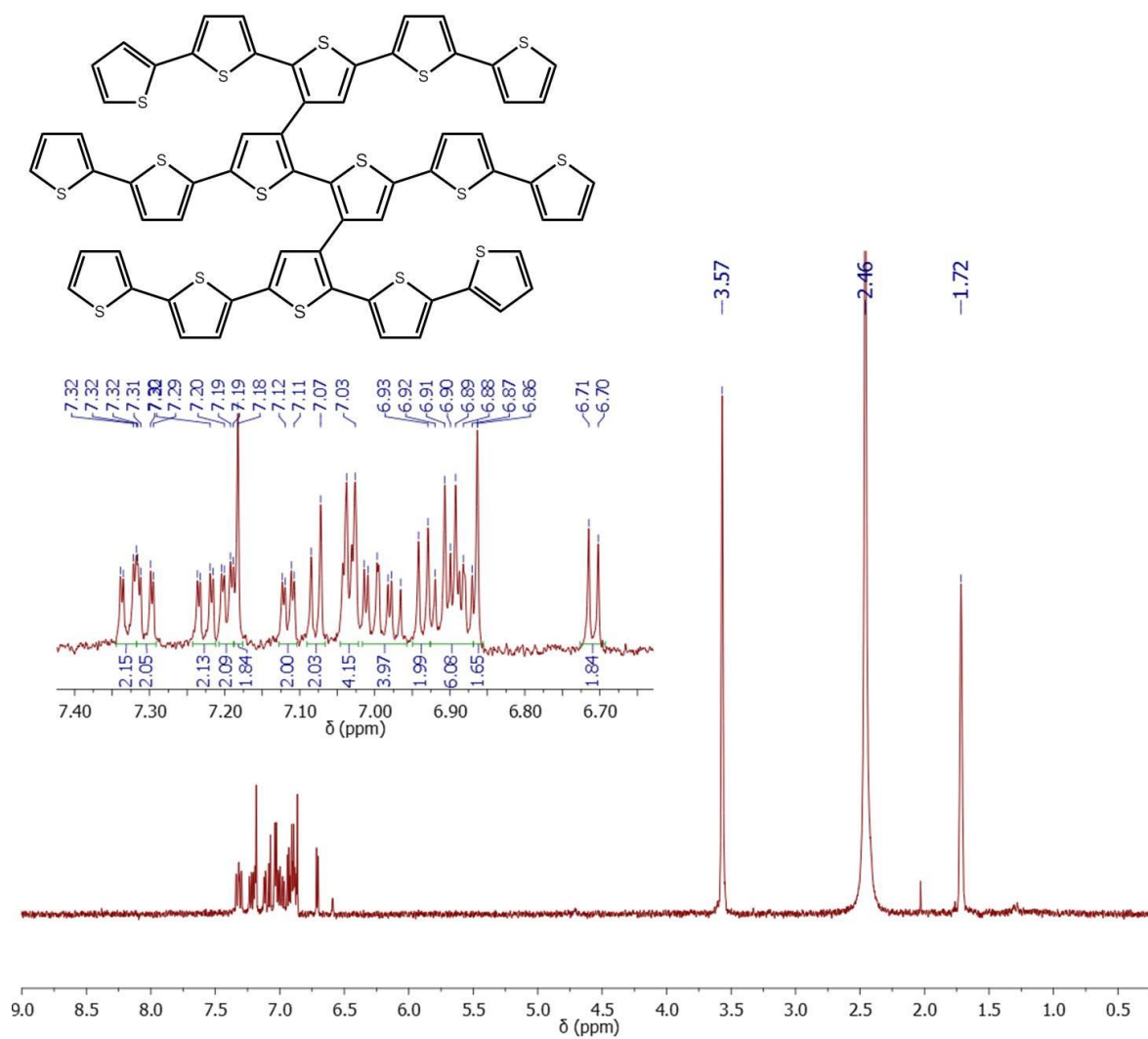


Figure S9. ^1H NMR spectrum of SCT-2 in THF- d_8 .

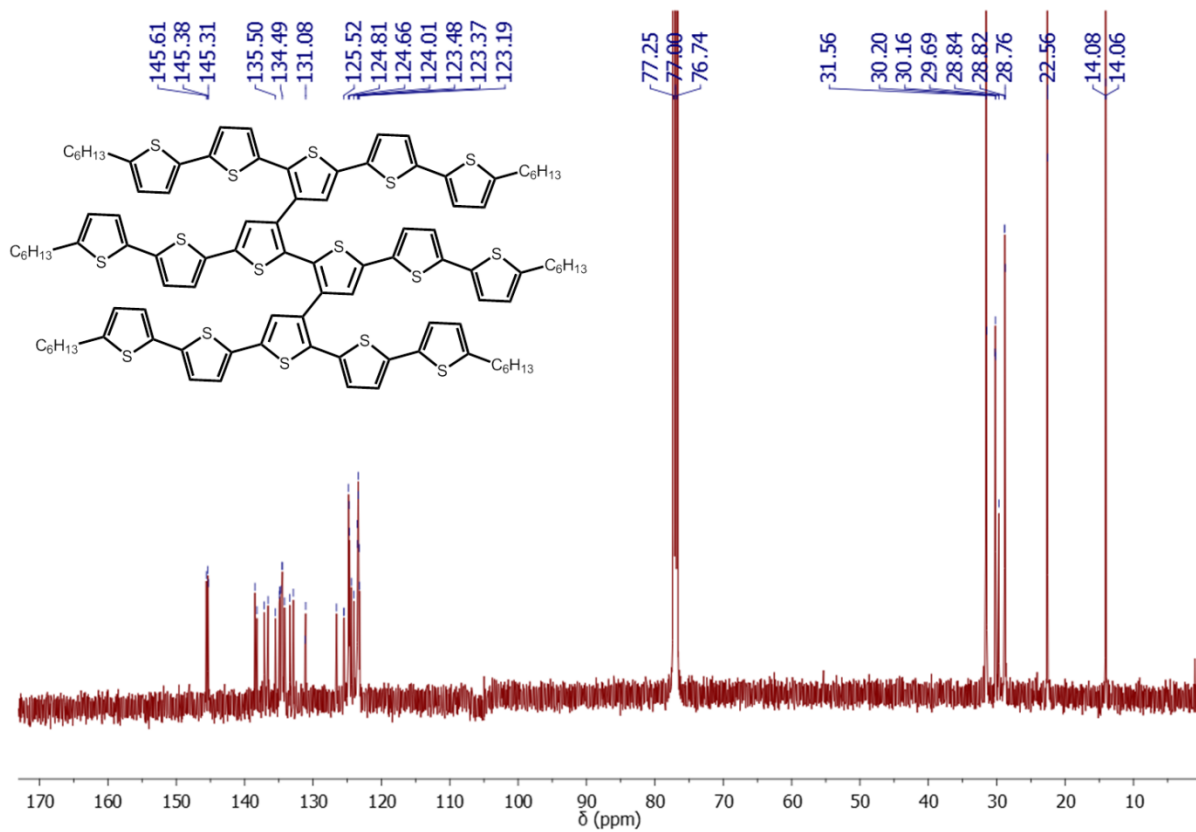


Figure S12. ^{13}C NMR spectrum of **SCT-3** in CDCl_3 .

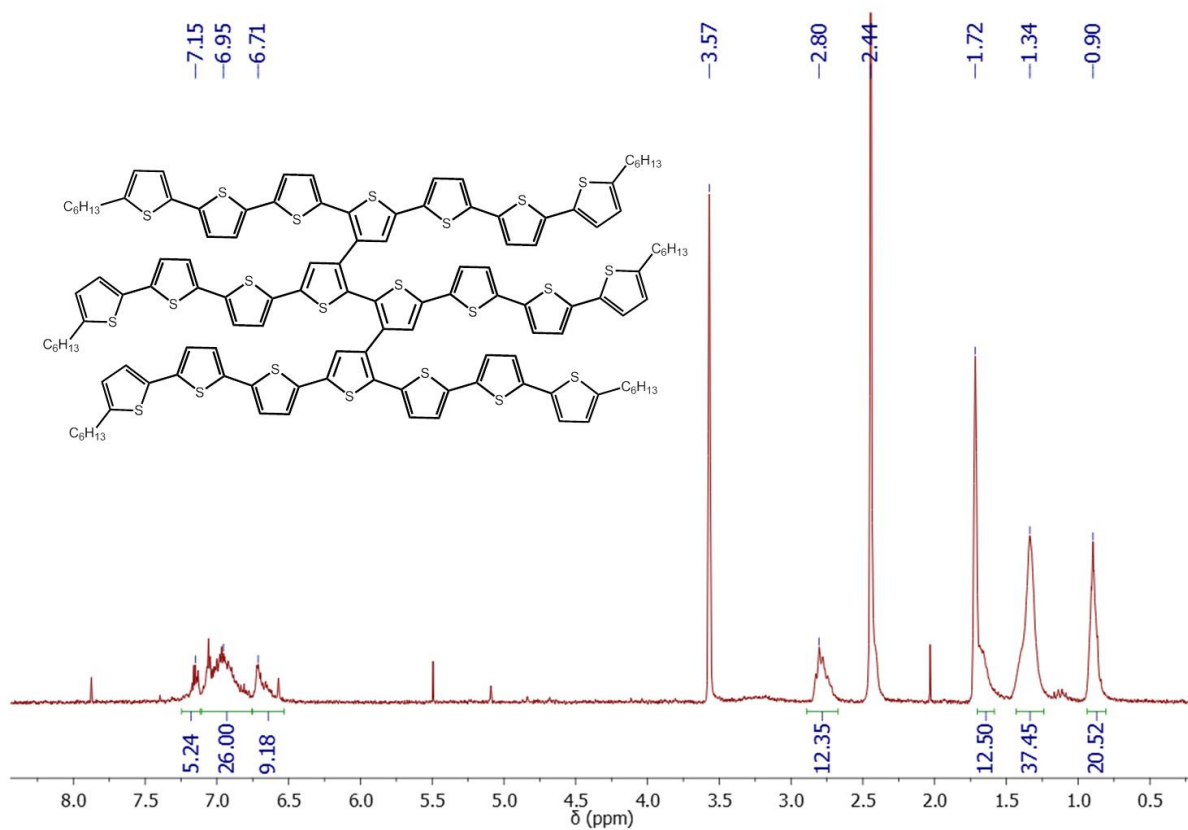
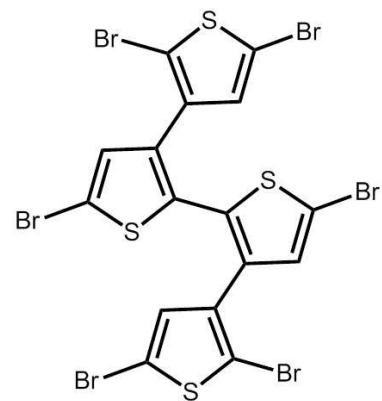


Figure S13. ^1H NMR spectrum of **SCT-4** in THF-d_8 .

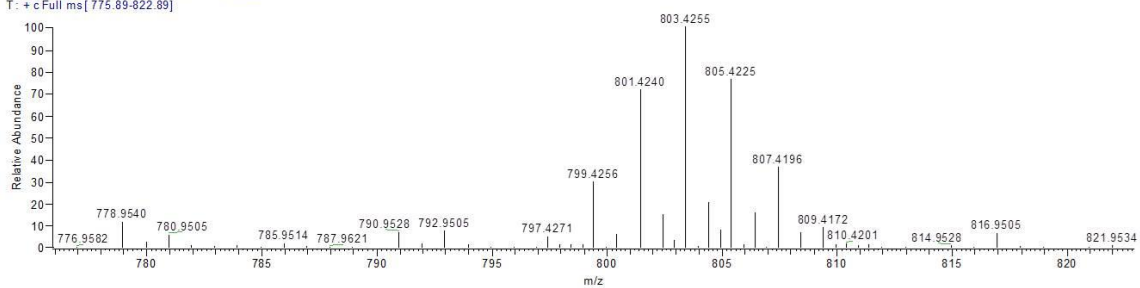


A:\PSG56-av-c1
study[.]

13/07/2014 11:21:11 AM

PSG56

PSG56-av-c1#1 RT: 2.05 AV: 1 NL: 149E6
T: + c Full ms [775.89-822.89]



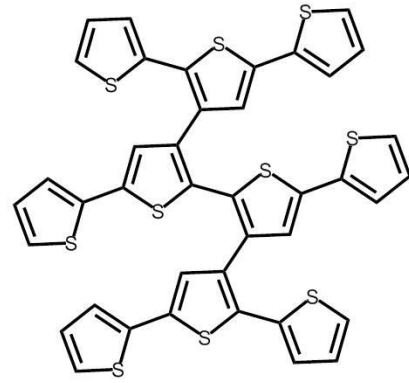
PSG56-av-c1#1 RT: 2.05

T: + c Full ms [775.89-822.89]

m/z= 797.07-809.63

m/z	Intensity	Relative	Theo. Mass	Delta (ppm)	RDB equiv.	Composition
797.4271	69985.0	4.71	797.4296	-3.11	12.0	C ₁₆ H ₄ ⁷⁹ Br ₆ ³² S ₄
799.4256	444023.0	29.86	799.4276	-2.45	12.0	C ₁₆ H ₄ ⁷⁹ Br ₅ ⁸¹ Br ₁ ³² S ₄
801.4240	1070471.0	71.98	801.4255	-1.85	12.0	C ₁₆ H ₄ ⁷⁹ Br ₄ ⁸¹ Br ₂ ³² S ₄
802.4313	225287.0	15.15	802.4333	-2.57	11.5	C ₁₆ H ₅ ⁷⁹ Br ₄ ⁸¹ Br ₂ ³² S ₄
803.4255	1487095.0	100.00	803.4235	2.56	12.0	C ₁₆ H ₄ ⁷⁹ Br ₃ ⁸¹ Br ₃ ³² S ₄
804.4264	302729.0	20.36	804.4313	-6.07	11.5	C ₁₆ H ₅ ⁷⁹ Br ₃ ⁸¹ Br ₃ ³² S ₄
805.4225	1135433.0	76.35	805.4214	1.38	12.0	C ₁₆ H ₄ ⁷⁹ Br ₂ ⁸¹ Br ₄ ³² S ₄
807.4196	543993.0	36.58	807.4194	0.26	12.0	C ₁₆ H ₄ ⁷⁹ Br ₁ ⁸¹ Br ₅ ³² S ₄

Figure S14. High resolution EI-MS spectrum of compound 3.

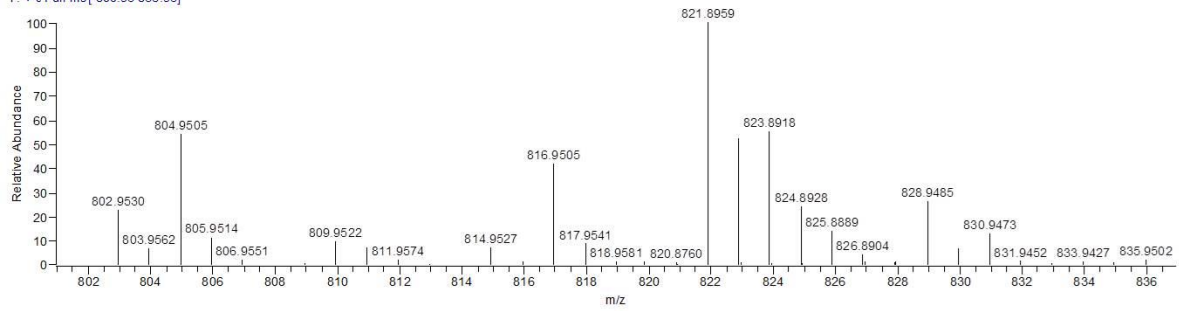


A:\PSG170-av-c2
study[.]

13/07/2014 10:48:09 AM

PSG170

PSG170-av-c2#1 RT: 6.17 AV: 1 NL: 3.82E5
T: + c Full ms [800.93-836.93]



PSG170-av-c2#1 RT: 6.17
T: + c Full ms [800.93-836.93]
m/z= 821.55-822.87

m/z	Intensity	Relative	Theo. Mass	Delta (ppm)	RDB equiv.	Composition
821.8959	381718.0	100.00	821.8929	3.69	30.0	C ₄₀ H ₂₂ ³² S ₁₀

Figure S15. High resolution EI-MS spectrum of **SCT-1**.

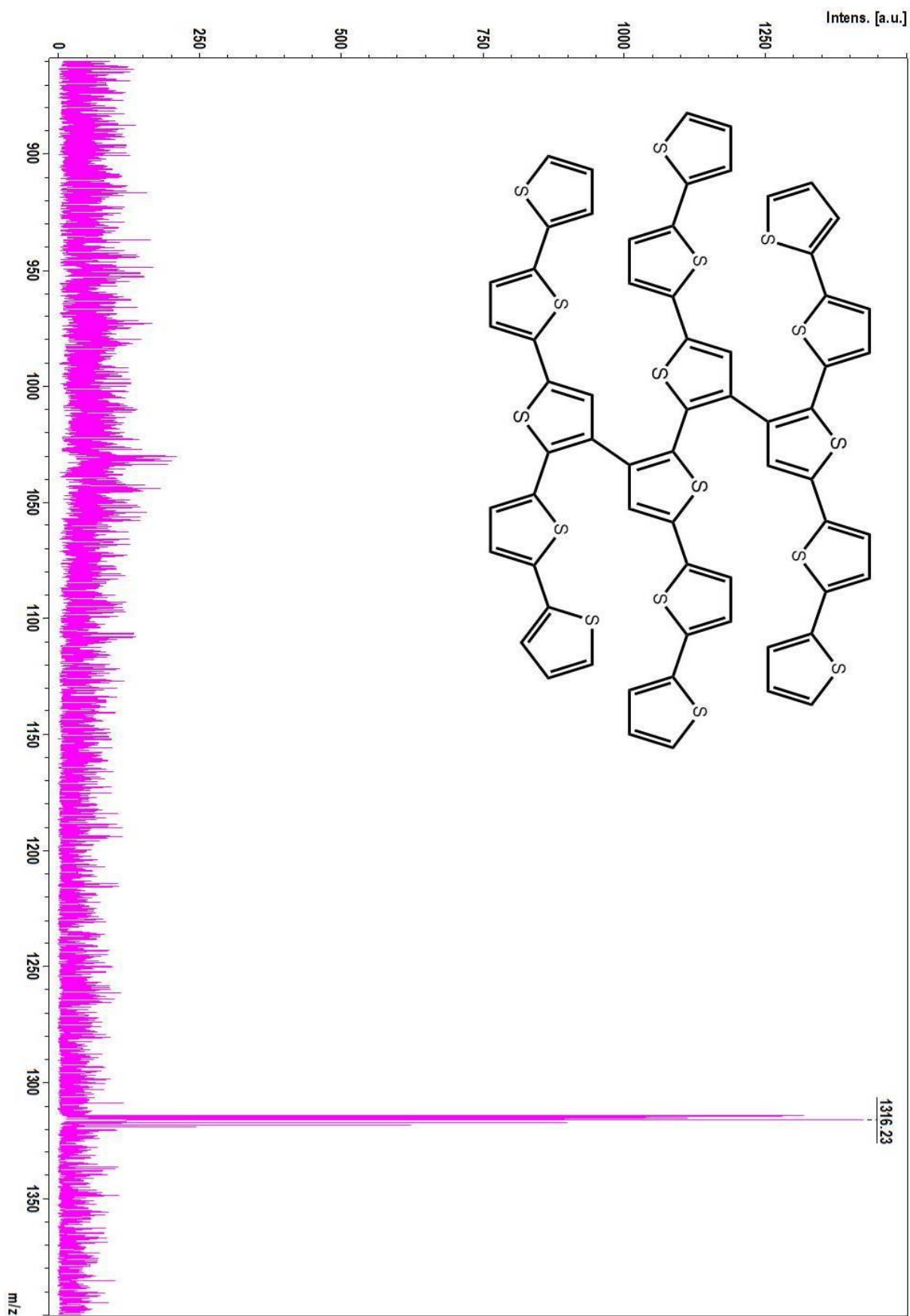


Figure S16. MALDI-TOF spectrum of SCT-2.

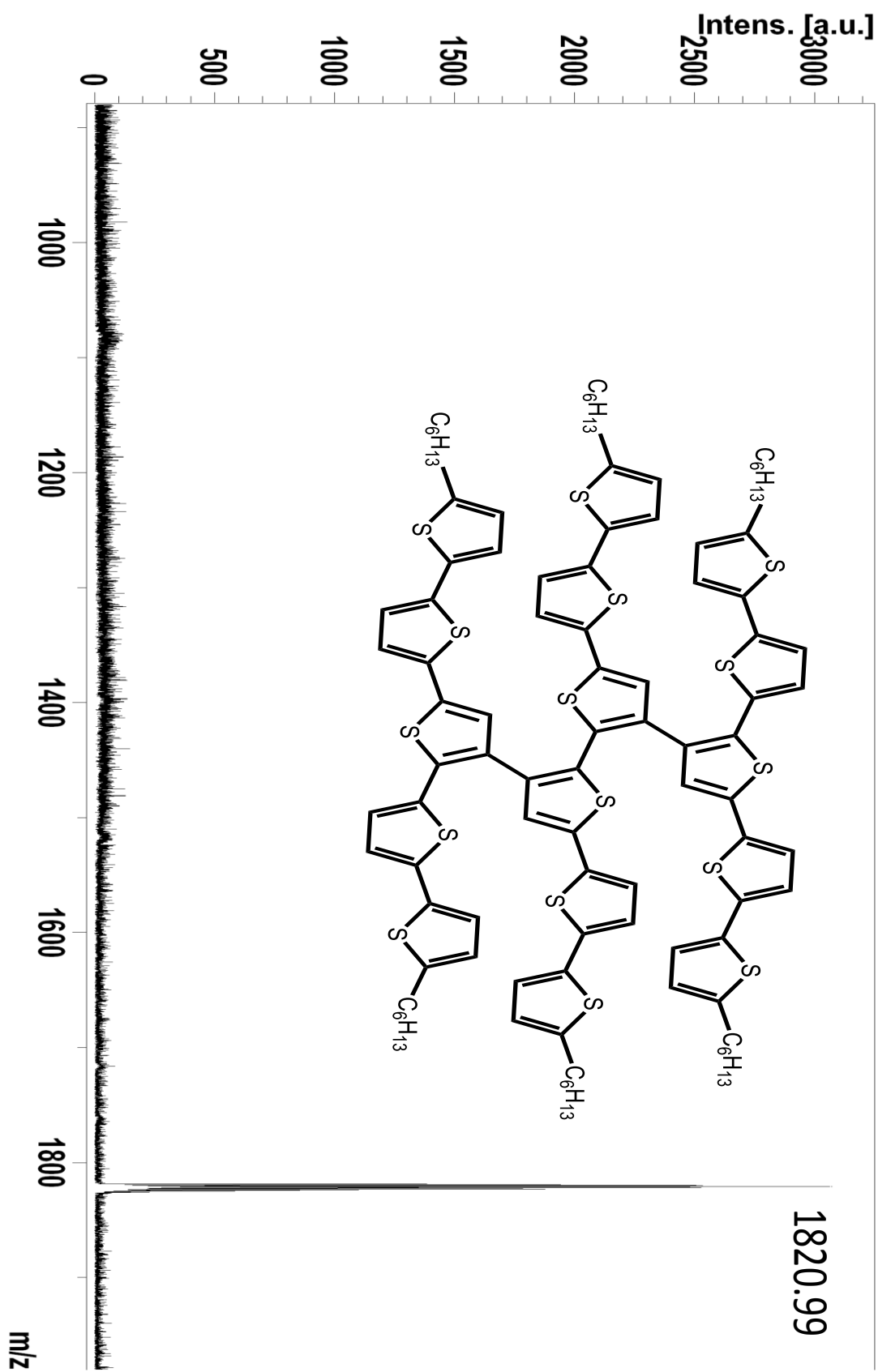


Figure S17. MALDI-TOF spectrum of SCT-3.

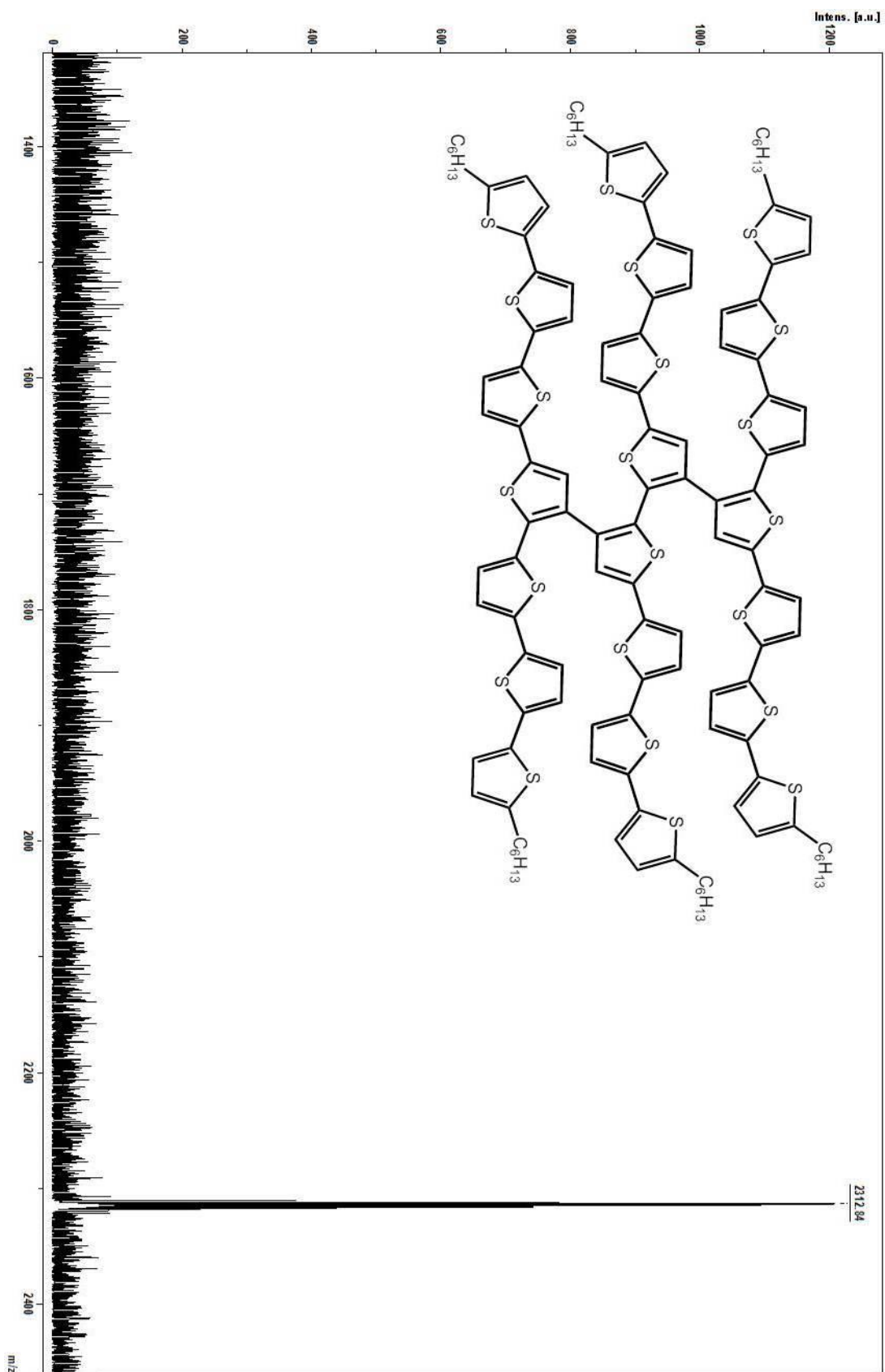
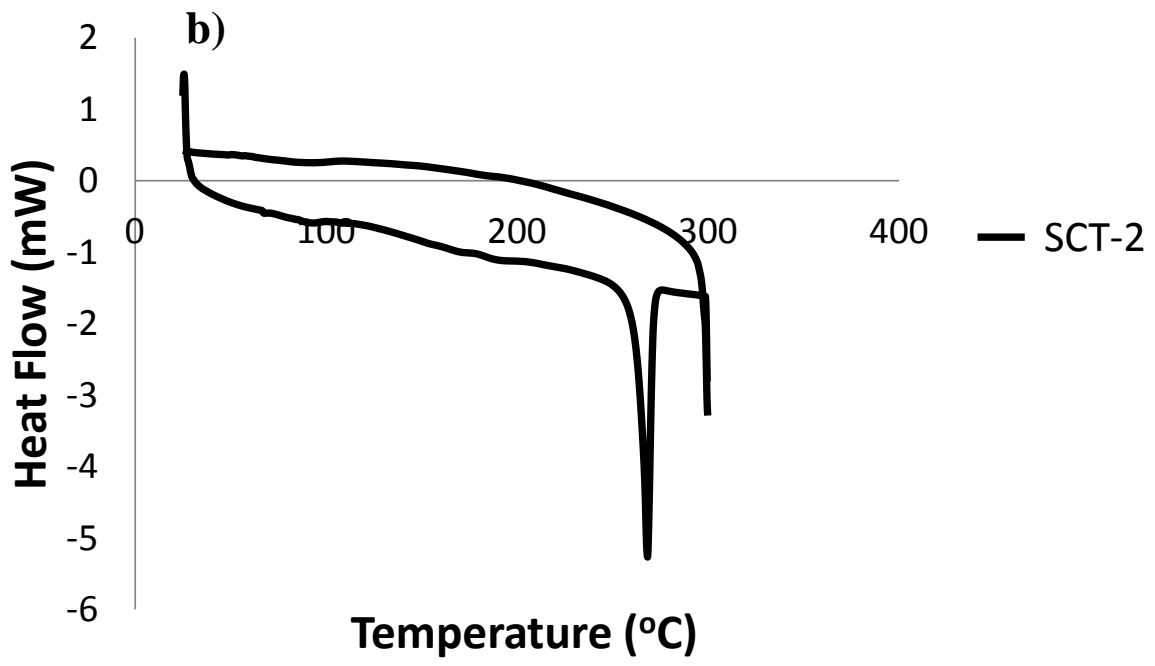
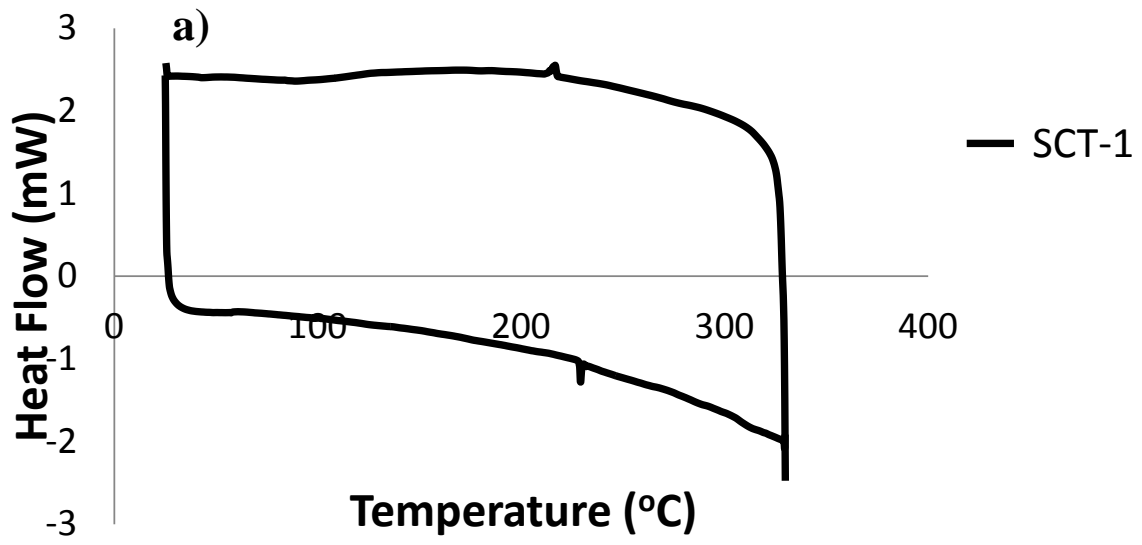


Figure S18. MALDI-TOF spectrum of SCT-4.

2.DSC results



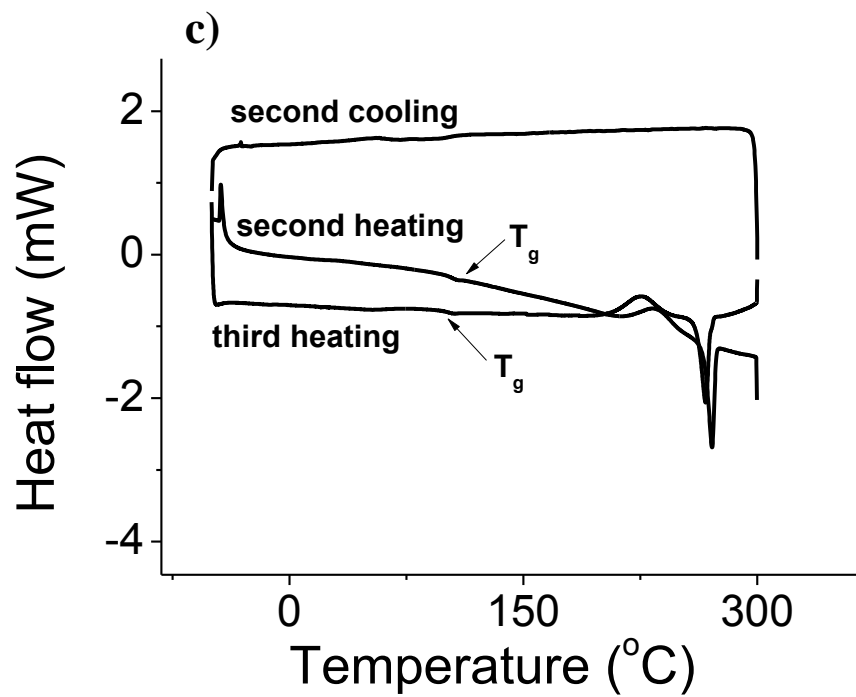


Figure S19. DSC curves of (a) **SCT-1** recorded at heating rate of $5\text{ }^{\circ}\text{C min}^{-1}$; (b) **SCT-2** (first heating, $10\text{ }^{\circ}\text{C min}^{-1}$) and (c) **SCT-2** (second heating and third heating, $5\text{ }^{\circ}\text{C min}^{-1}$)

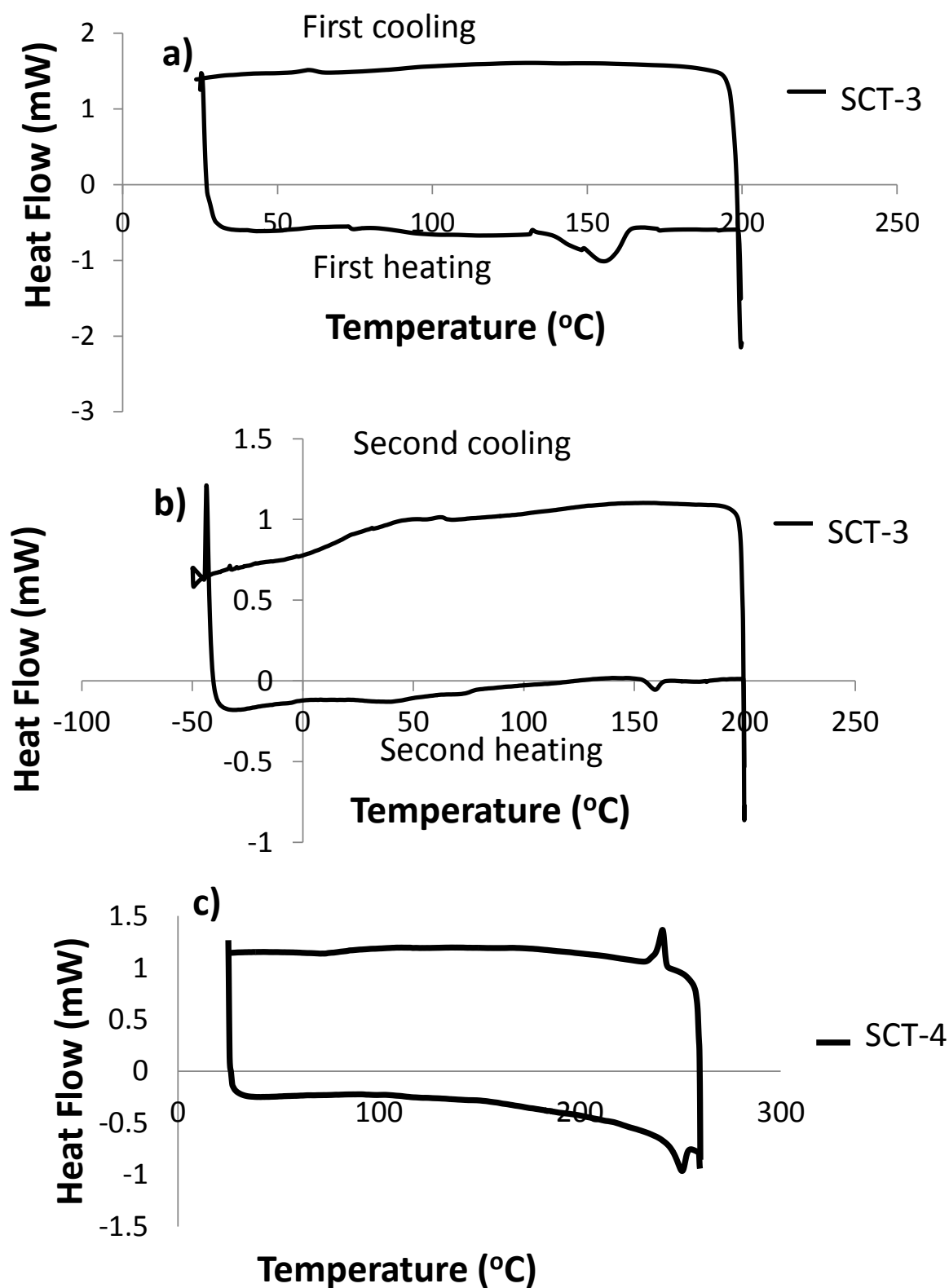


Figure S20. DSC curves of **SCT-3** for (a) first heating and (b) second heating; (c) **SCT-4** recorded at heating rate of $5\text{ }^{\circ}\text{C min}^{-1}$ under nitrogen atmosphere.

3. Optimized structures and frontier orbital plots of SCTs from DFT calculation at B3LYP/6-31G(d) level using Gaussian09.¹

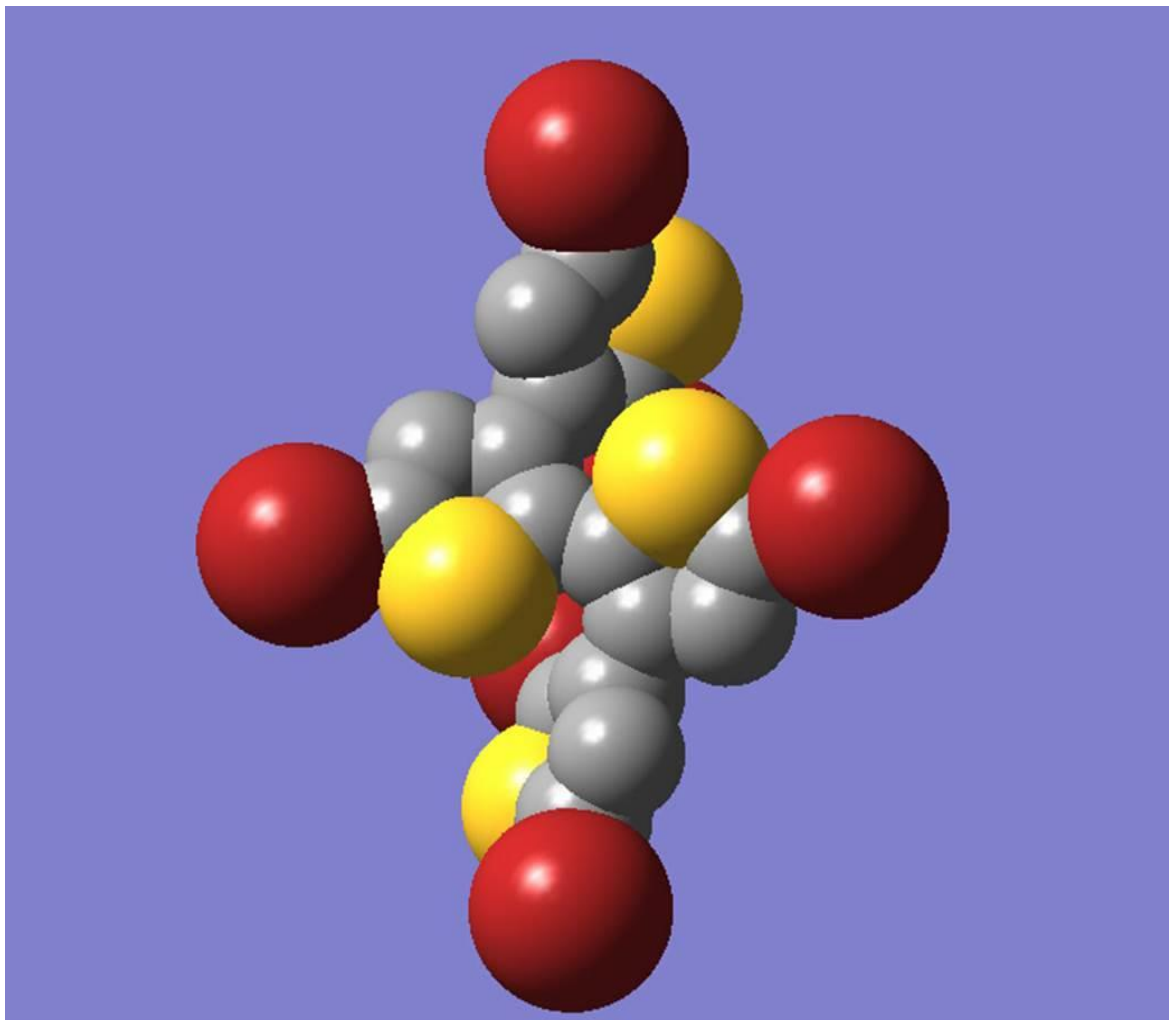


Figure S21. Optimized structure of **3** obtained from DFT calculation at B3LYP/6-31G (d) level with omitted hydrogen atoms for better clarity.

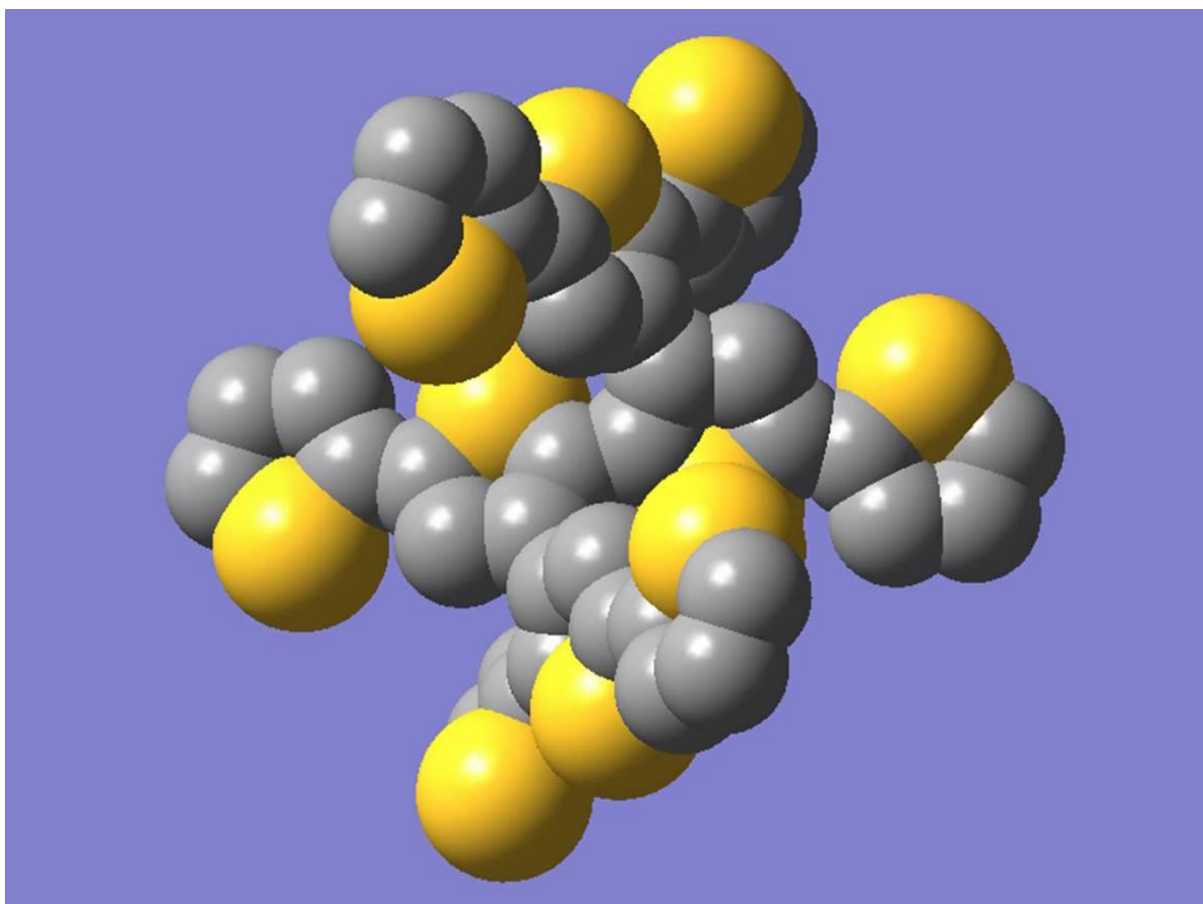


Figure S22. Optimized structure of **SCT-1** obtained from DFT calculation at B3LYP/6-31G (d) level with omitted hydrogen atoms for better clarity.

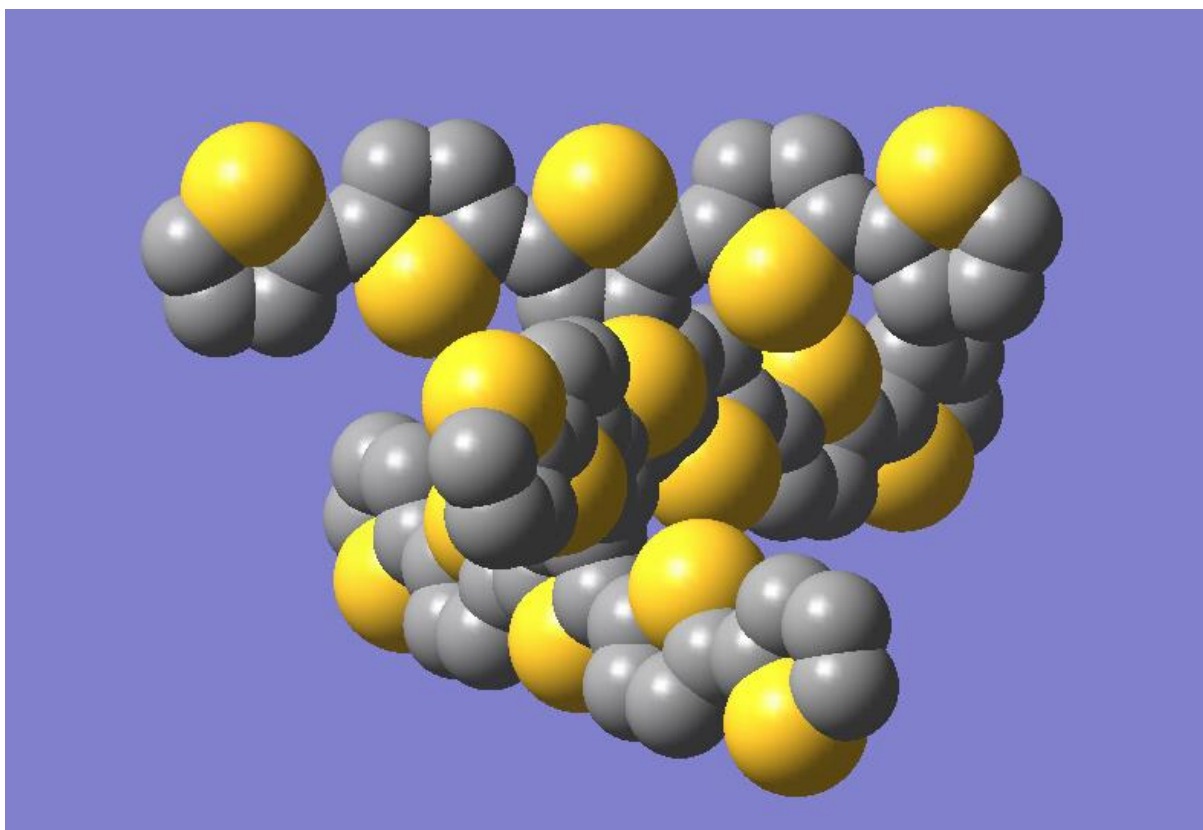


Figure S23. Optimized structure of **SCT-2** obtained from DFT calculation at B3LYP/6-31G (d) level with omitted hydrogen atoms for better clarity.

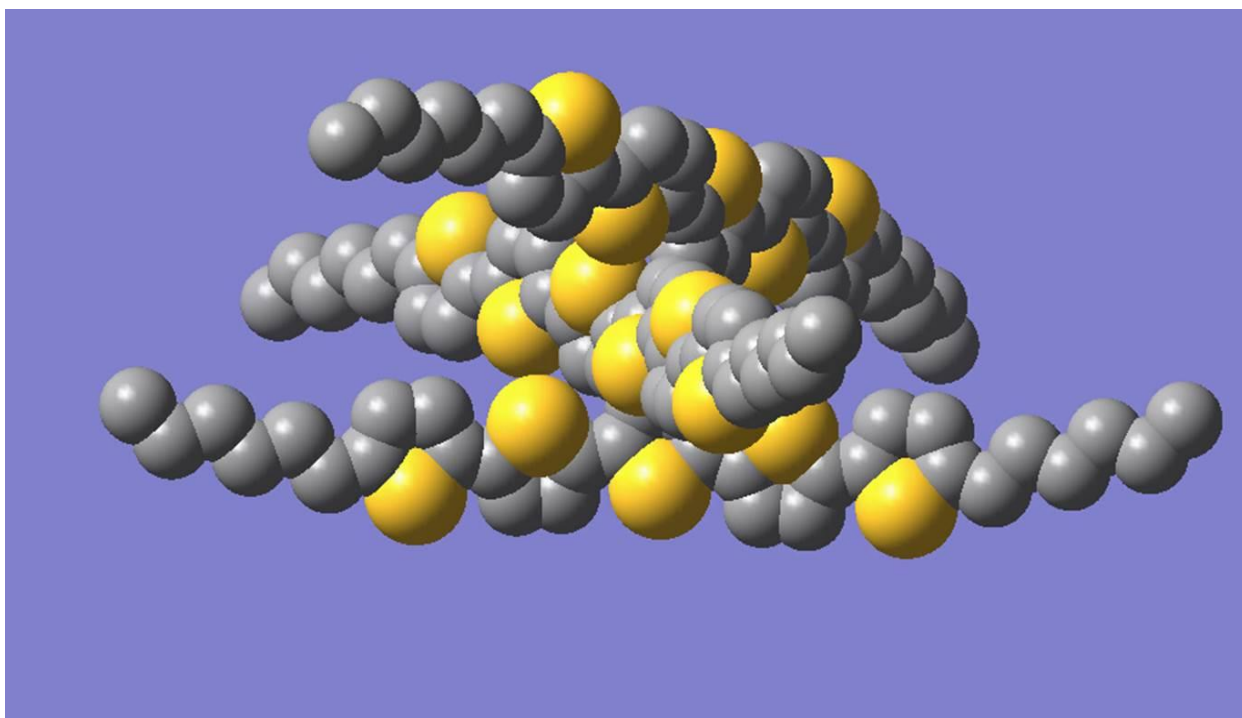


Figure S24. Optimized structure of **SCT-3** obtained from DFT calculation at B3LYP/6-31G (d) level with omitted hydrogen atoms for better clarity.

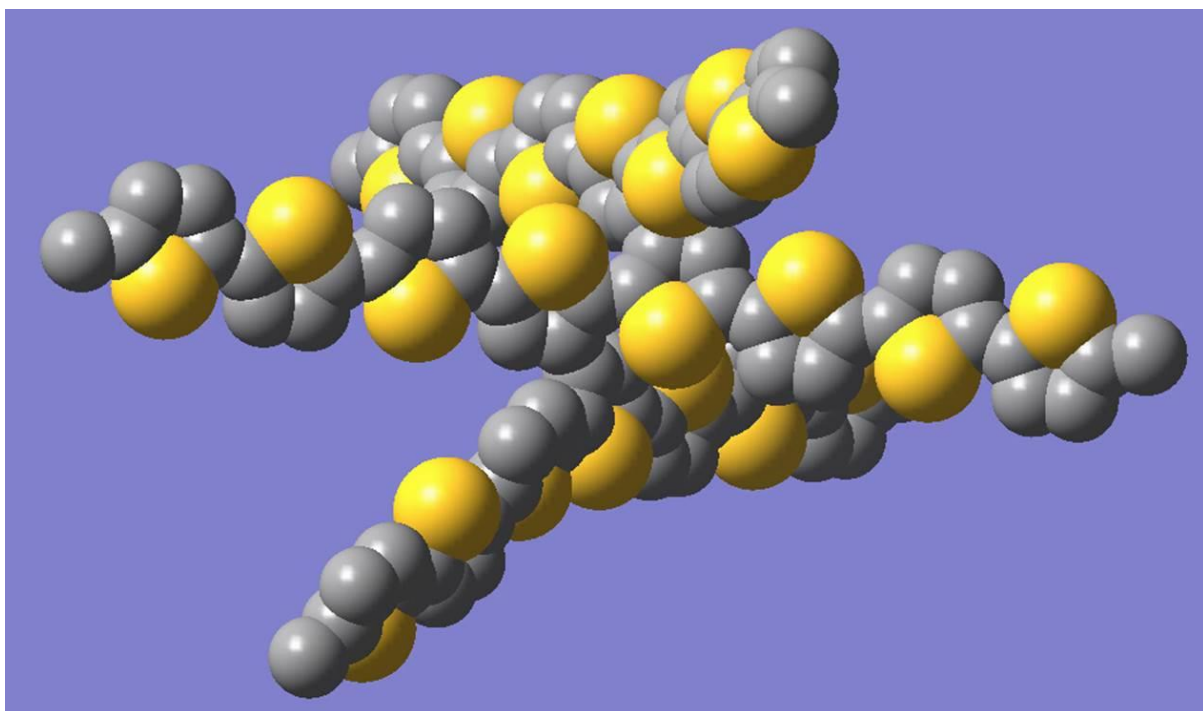


Figure S25. Optimized structure of **SCT-4** obtained from DFT calculation at B3LYP/6-31G(d) level with omitted hydrogen atoms for better clarity.

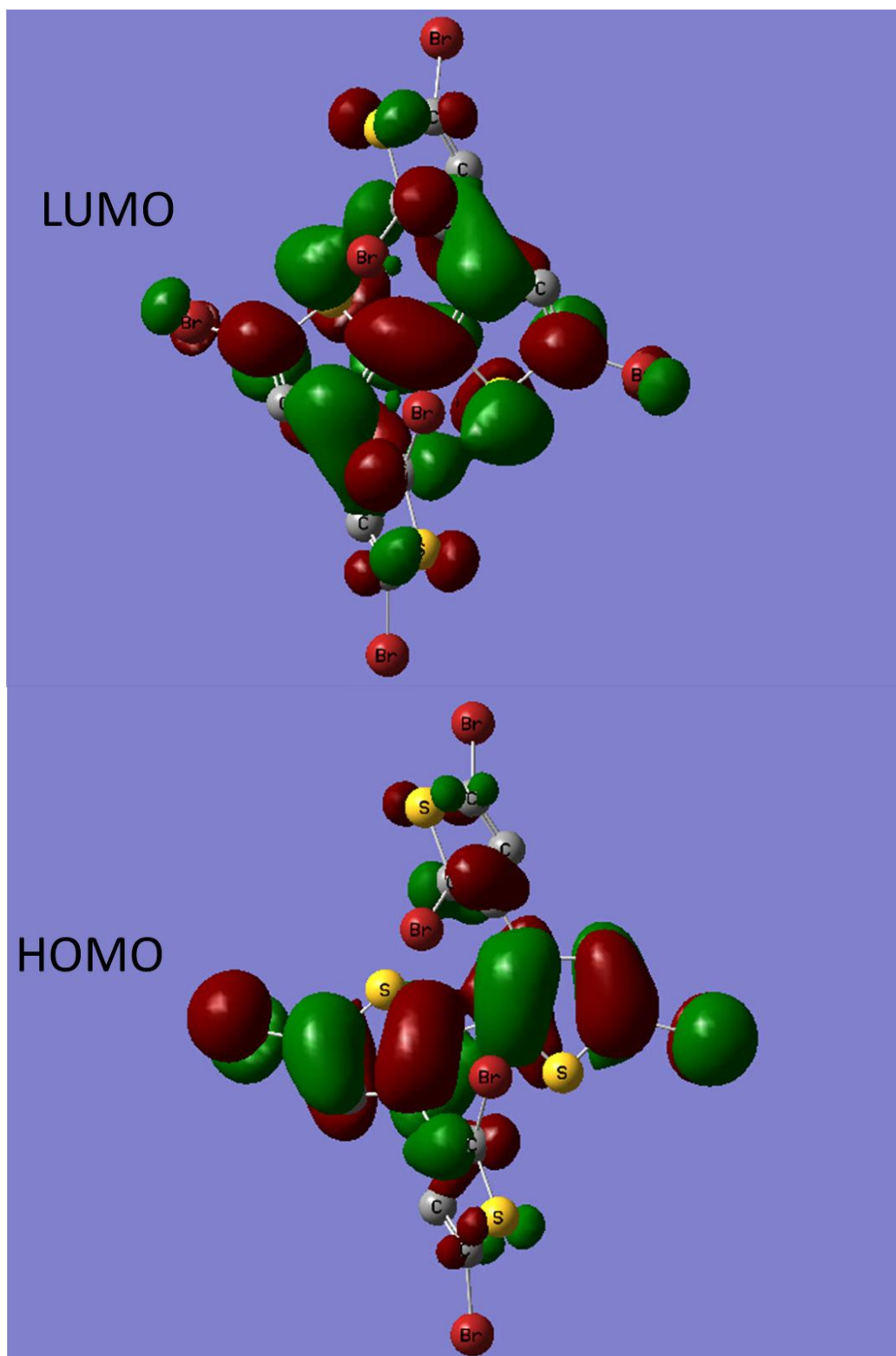


Figure S26. Frontier orbitals of compound **3** obtained from DFT calculation at B3LYP/6-31G (d) level with omitted hydrogen atoms for better clarity.

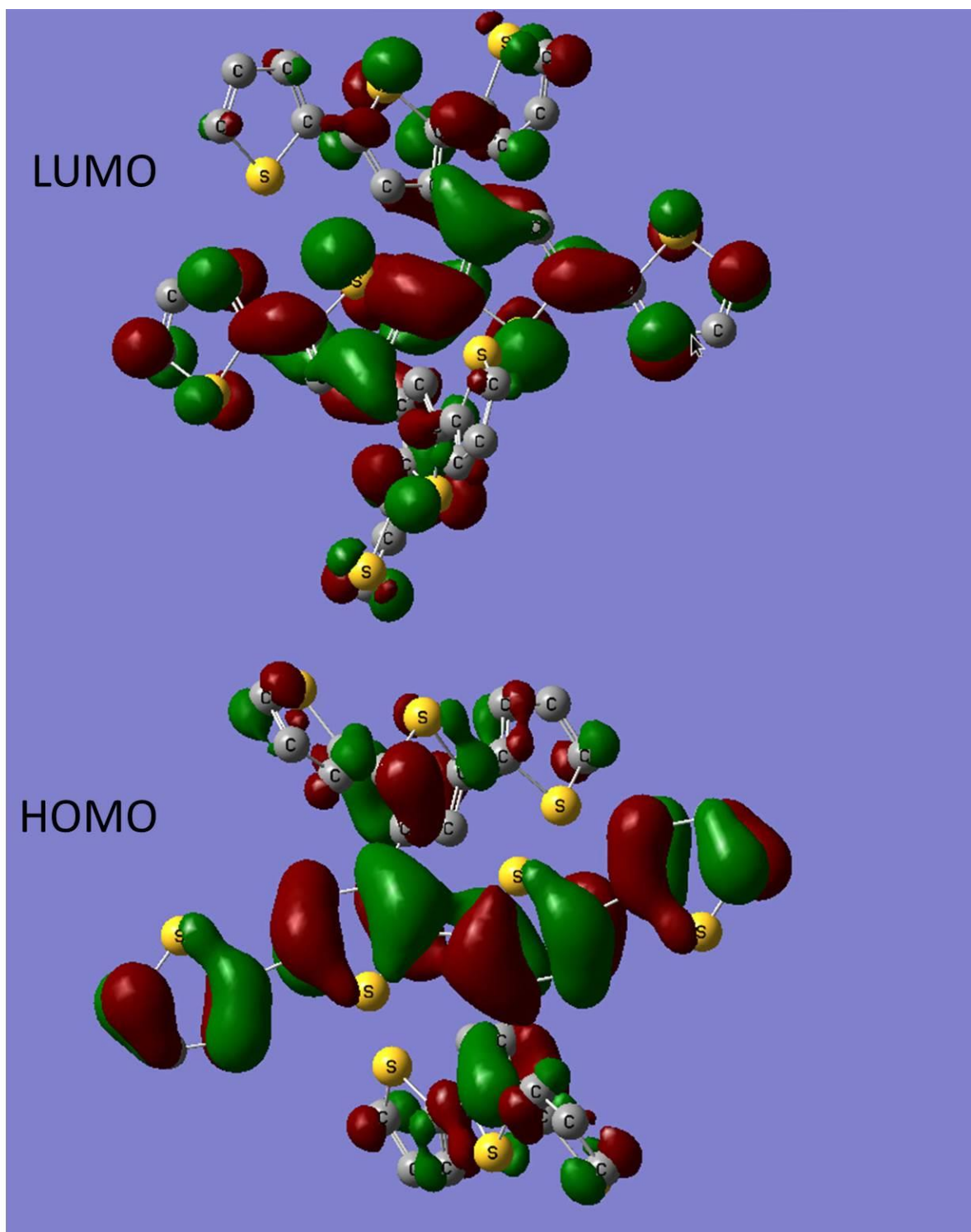


Figure S27. Frontier orbitals of **SCT-1** obtained from DFT calculation at B3LYP/6-31G (d) level with omitted hydrogen atoms for better clarity.

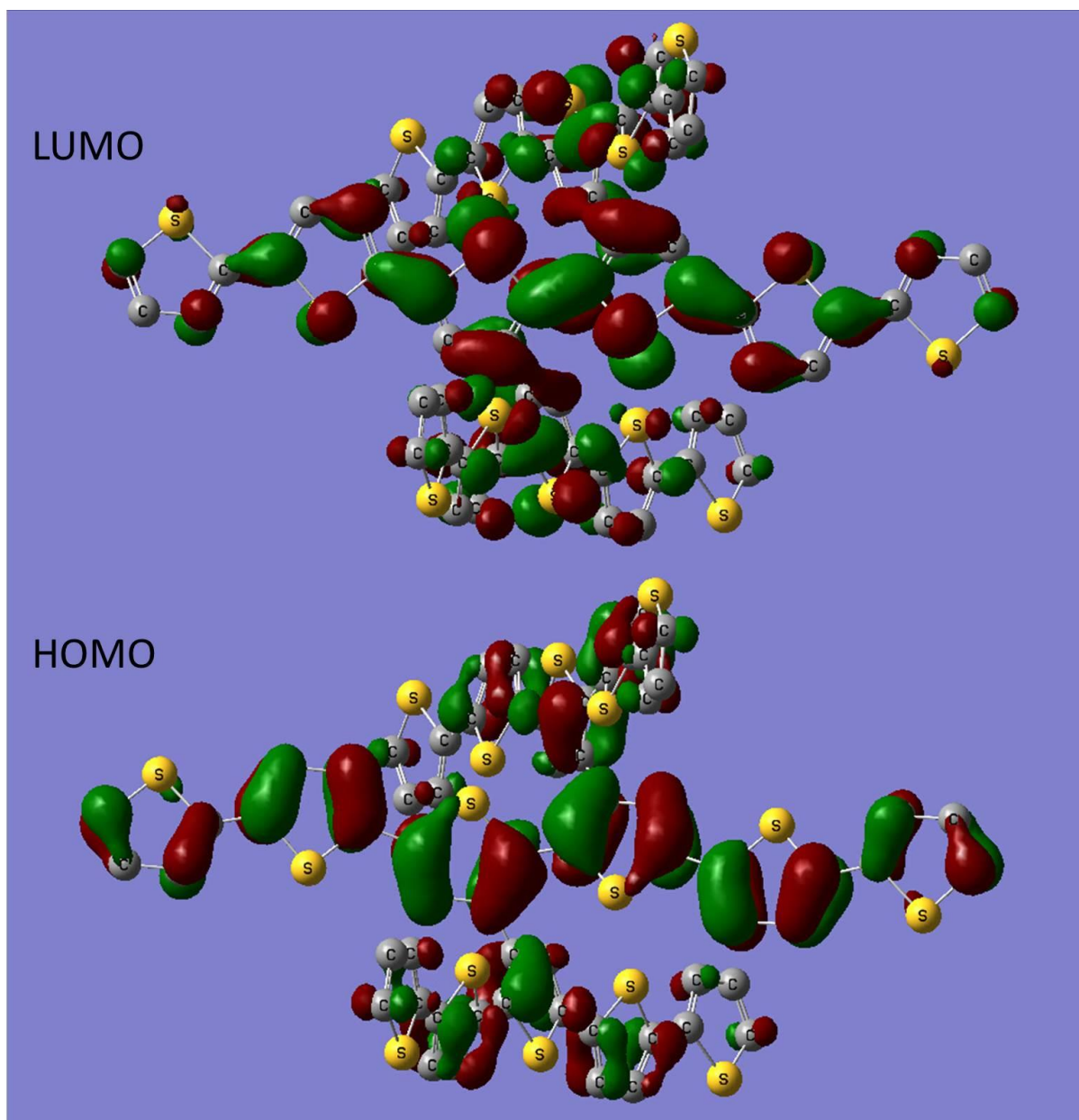


Figure S28. Frontier orbitals of SCT-2 obtained from DFT calculation at B3LYP/6-31G (d) level with omitted hydrogen atoms for better clarity.

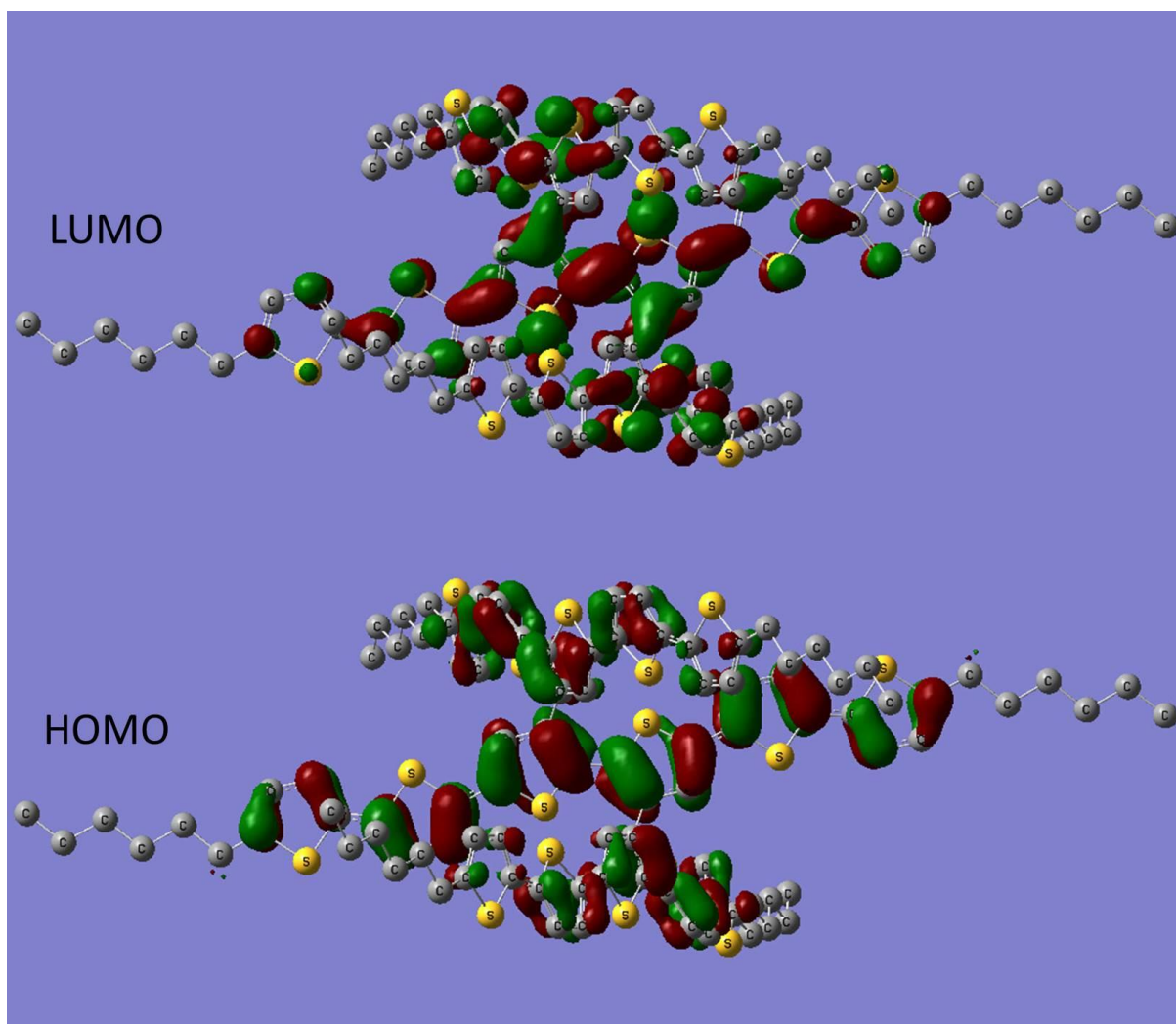


Figure S29. Frontier orbitals of **SCT-3** obtained from DFT calculation at B3LYP/6-31G (d) level with omitted hydrogen atoms for better clarity.

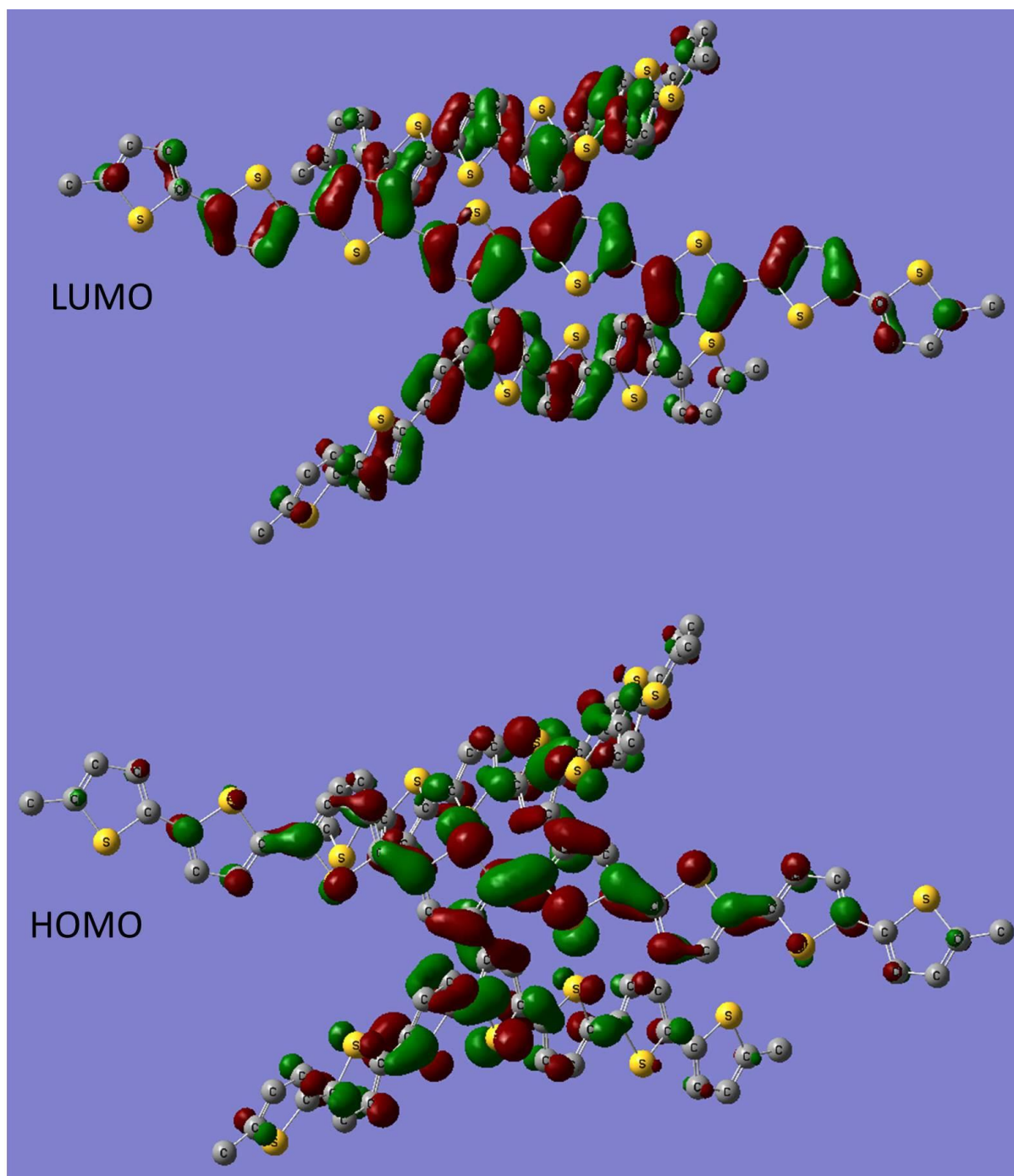


Figure S30. Frontier orbitals of **SCT-4** obtained from DFT calculation at B3LYP/6-31G(d) level with omitted hydrogen atoms for better clarity.

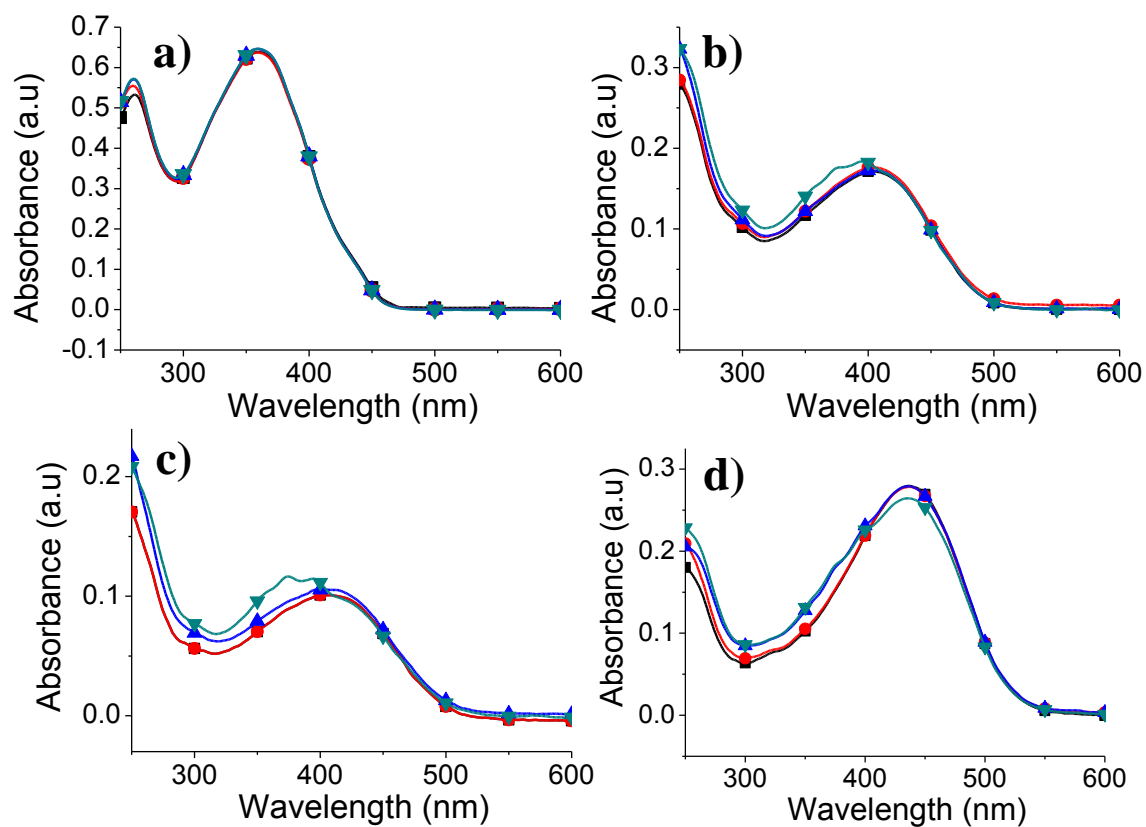


Figure S31. Absorption spectra of **SCT-1** (a), **SCT-2** (b), **SCT-3** (c), and **SCT-4** (d) before light irradiation (-■-), 6 hours (-●-), 12 hours (-▲-), and 24 hours (-▼-) after light irradiation in dilute THF.

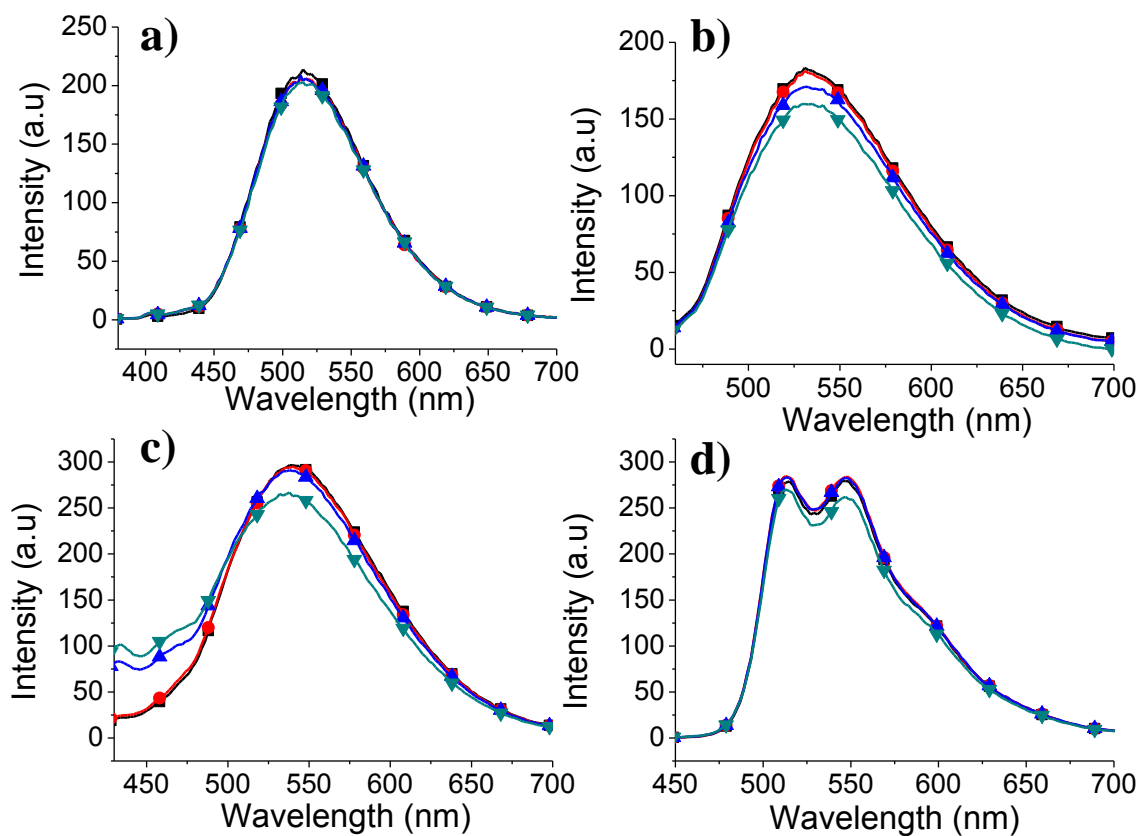


Figure S32. Emission spectra of **SCT-1** (a), **SCT-2** (b), **SCT-3** (c), and **SCT-4** (d) before light irradiation (-■-), 6 hours (-●-), 12 hours (-▲-), and 24 hours (-▼-) after light irradiation in dilute THF.

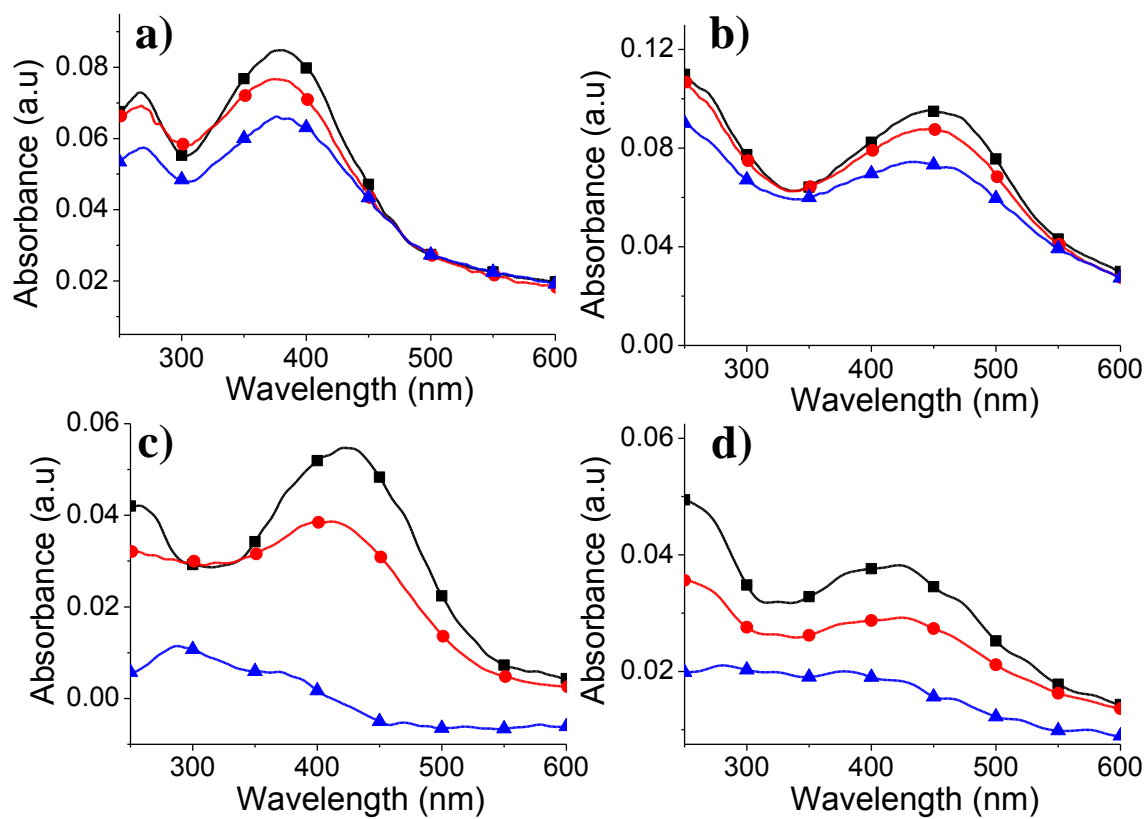


Figure S33. Absorption spectra of **SCT-1** (a), **SCT-2** (b), **SCT-3** (c), and **SCT-4** (d) thin films before light irradiation (-■-), 12 hours (-●-), and 24 hours (-▲-) after light irradiation. The **SCTs** thin films were prepared by spin casting the **SCTs** solution in THF at room temperature.

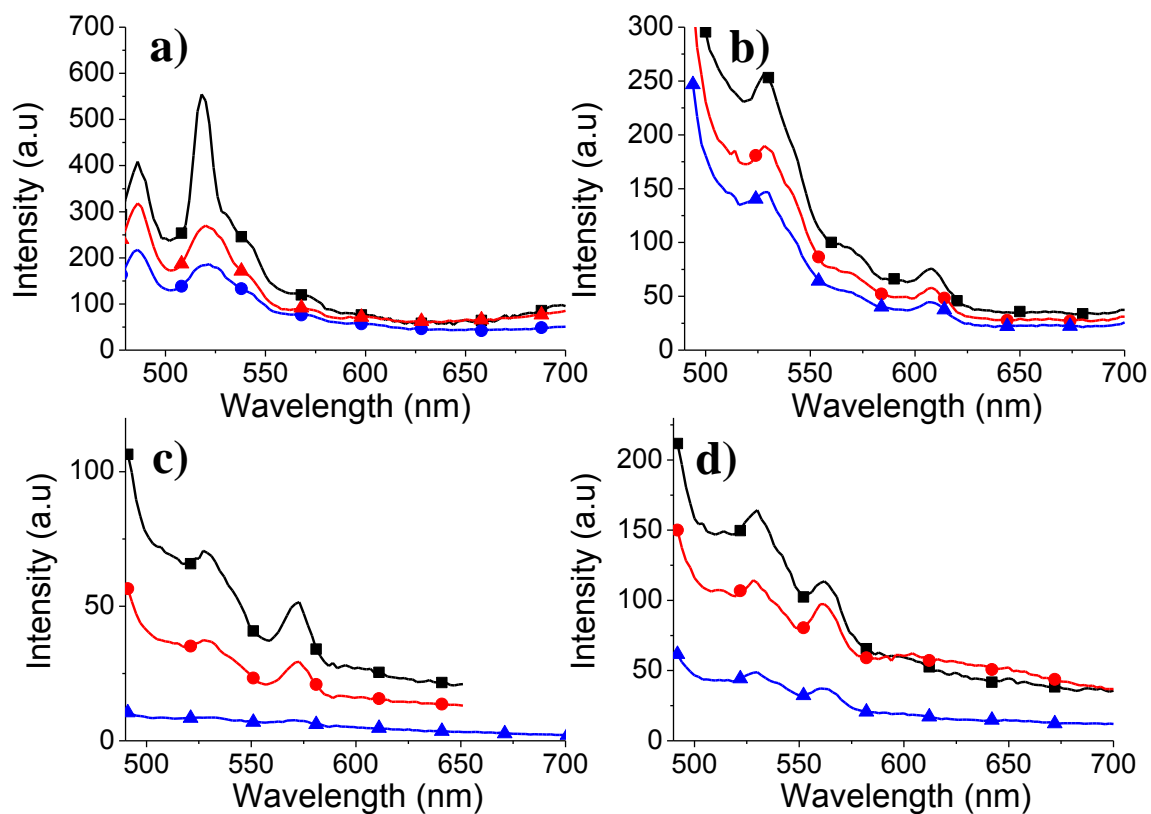


Figure S34. Emission spectra of **SCT-1** (a), **SCT-2** (b), **SCT-3** (c), and **SCT-4** (d) thin films before light irradiation (-■-), 12 hours (-●-), and 24 hours (-▲-) after light irradiation. The **SCTs** thin films were prepared by spin casting the **SCTs** solution in THF at room temperature.

4. Absorption and emission spectra of SCTs in presence of Pb(II) and Cd(II) ions.

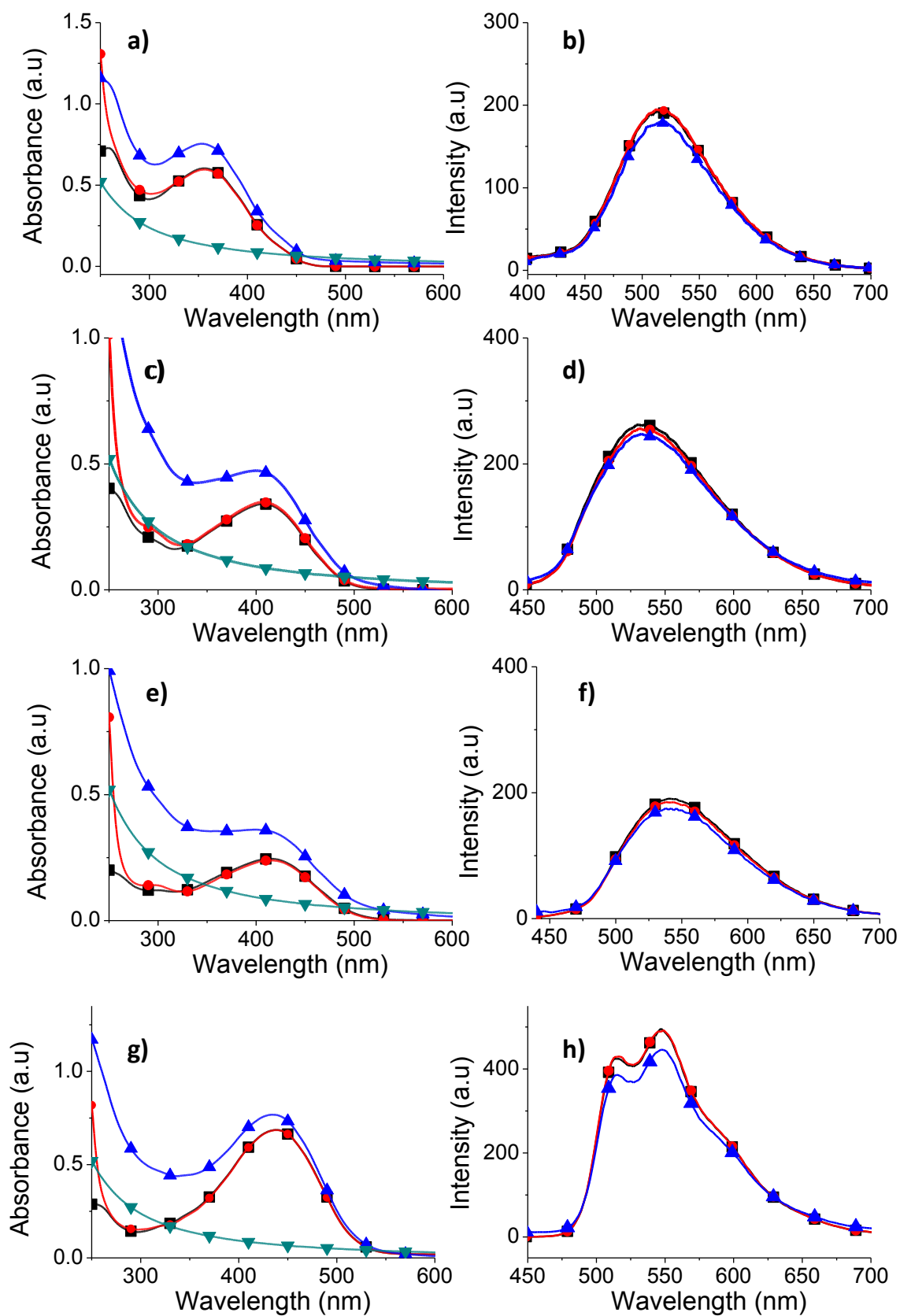


Figure S35. Absorption and emission spectra of **SCT-1** (a, b), **SCT-2** (c, d), **SCT-3** (e, f) and **SCT-4** (g, h) in presence of Pb(II) and Cd(II) ions; SCTs in THF (-■-), in presence of 1×10^{-4}

3×10^{-3} M $\text{Pb}(\text{NO}_3)_2$ aqueous solution (-●-), and in presence of 1×10^{-3} M $\text{Cd}(\text{CH}_3\text{CO}_2)_2$ aqueous solution (-▲-). The absorption spectra of 1×10^{-3} M $\text{Cd}(\text{CH}_3\text{CO}_2)_2$ in THF was shown (-▼-). The concentrations of **SCT-1**, **SCT-2**, **SCT-3**, and **SCT-4** are 1.5×10^{-5} M, 3.4×10^{-6} M, 2.4×10^{-6} M, and 4.7×10^{-6} M, respectively.

5. Absorption spectra of SCT-4 at pH 1 - 6

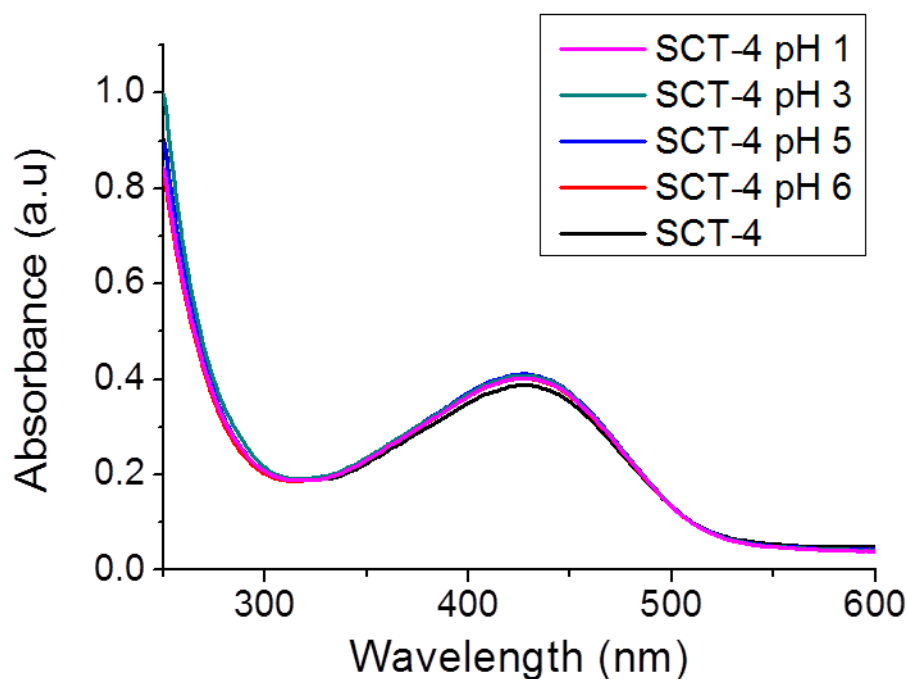


Figure S36. Uv-visible absorption of **SCT-4** at different acidic pH (pH 1 – 6) in THF and appropriate amounts of dilute HCl was added to get the desired pH.

6. SEM micrographs on SCT/Hg(II) and SCT/TCNQ complexes

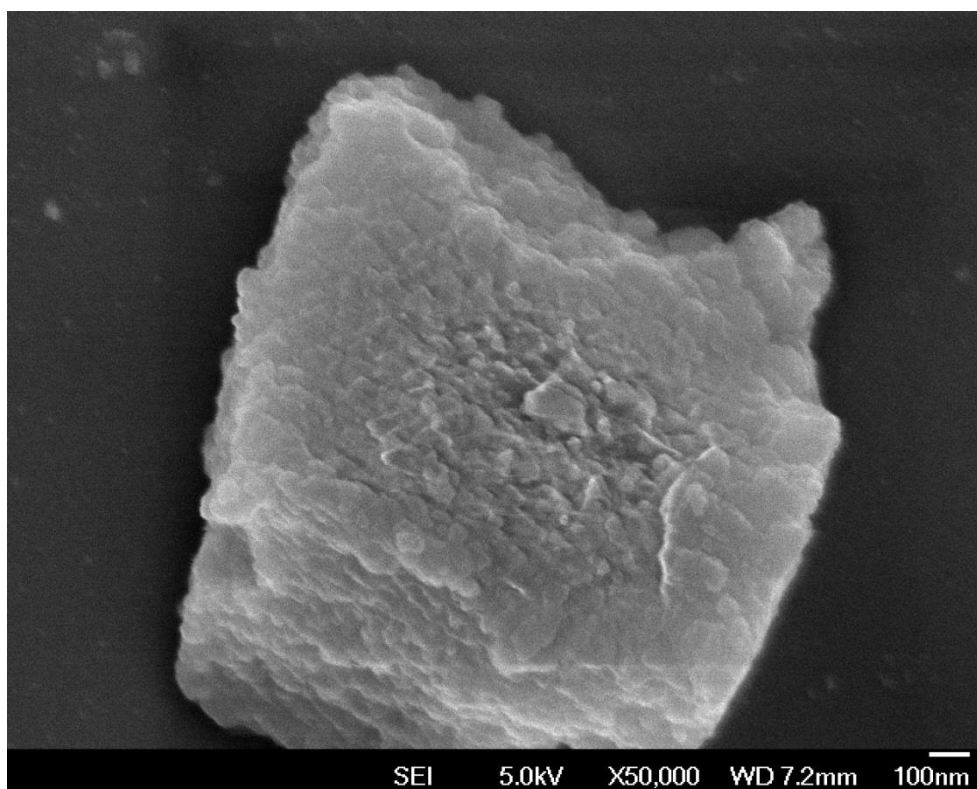


Figure S37. SEM micrograph on the Hg(II)-SCTs precipitate by dropcasting on the glass substrate and dried under ambient condition before examination by FESEM.

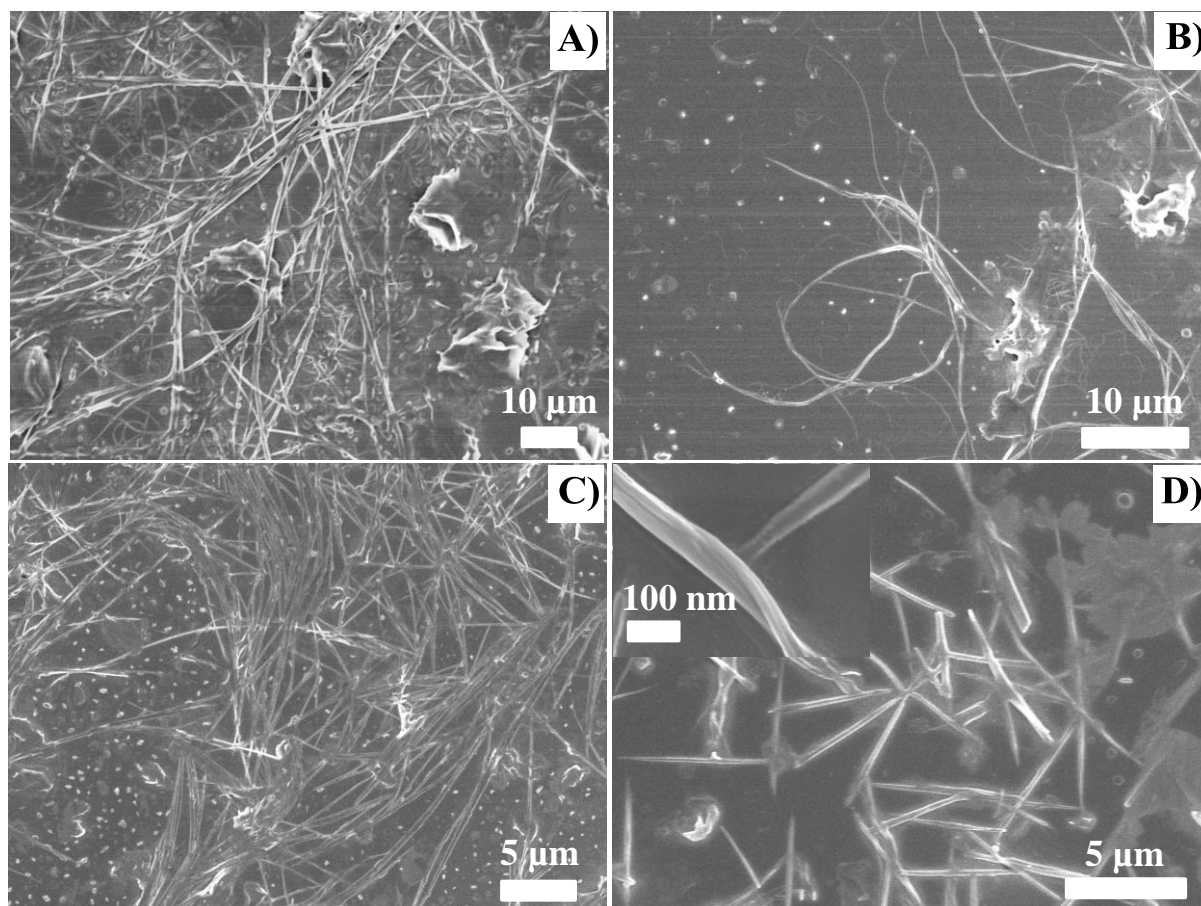


Figure S38 Field emission SEM micrographs (a) **SCT-1**, (b) **SCT-2**, (c) **SCT-3** and (d) **SCT-4** with TCNQ; inset: magnified image on the SCT-4/TCNQ needle. The samples were prepared by dropcasting SCTs-TCNQ in THF on glass substrate and dried at ambient temperature prior to FESEM examination.

7. Theoretical calculations on HOMO energy levels of SCTs.

Table S1. Summary of electrochemical properties and of **SCT-1**, **SCT-2**, **SCT-3** and **SCT-4**.

	HOMO ^a (eV)	LUMO ^b (eV)	HOMO ^c (eV)	LUMO ^c (eV)	E_g^c (eV)
SCT-1	-5.28	-2.55	-5.05	-1.80	3.25
SCT-2	-5.26	-2.78	-4.83	-2.07	2.76

SCT-3	-5.22	-2.77	-4.64	-1.91	2.74
SCT-4	-5.07	-2.75	-4.65	-2.13	2.52

^a Electrochemical HOMO = $-(E^{\text{ox}} + 4.8)$ eV, where E^{ox} were determined from the onset potentials of first oxidation peak calibrated with ferrocene/ferrocenium ion redox couple in thin film. ^b LUMO = HOMO + optical band gap. ^c Theoretical calculations using DFT.

Reference

1. M. J. Frisch, G. W. Trucks, H. B. Schlegel, G. E. Scuseria, M. A. Robb, J. R. Cheeseman, G. Scalmani, V. Barone, B. Mennucci, G. A. Petersson, H. Nakatsuji, M. Caricato, X. Li, H. P. Hratchian, A. F. Izmaylov, J. Bloino, G. Zheng, J. L. Sonnenberg, M. Hada, M. Ehara, K. Toyota, R. Fukuda, J. Hasegawa, M. Ishida, T. Nakajima, Y. Honda, O. Kitao, H. Nakai, T. Vreven, J. A. Montgomery Jr., J. E. Peralta, F. Ogliaro, M. J. Bearpark, J. Heyd, E. N. Brothers, K. N. Kudin, V. N. Staroverov, R. Kobayashi, J. Normand, K. Raghavachari, A. P. Rendell, J. C. Burant, S. S. Iyengar, J. Tomasi, M. Cossi, N. Rega, N. J. Millam, M. Klene, J. E. Knox, J. B. Cross, V. Bakken, C. Adamo, J. Jaramillo, R. Gomperts, R. E. Stratmann, O. Yazyev, A. J. Austin, R. Cammi, C. Pomelli, J. W. Ochterski, R. L. Martin, K. Morokuma, V. G. Zakrzewski, G. A. Voth, P. Salvador, J. J. Dannenberg, S. Dapprich, A. D. Daniels, Ö. Farkas, J. B. Foresman, J. V. Ortiz, J. Cioslowski and D. J. Fox, **Gaussian 09**, revision **A.02**; Gaussian, Inc., Wallingford, CT, USA, **2009**.